

1 Investigation on Groundwater Velocity Based on the Finite Line 2 Heat Source Seepage Model

3 Wenke Zhang ^{a, b, *}, Hongxing Yang^b, Xiaoqiang Guo^c, Mingzhi Yu^a, Zhaohong Fang^a
4

5a. Department of Thermal Engineering, Shandong Jianzhu University, Jinan, China

6b. Renewable Energy Research Group, The Hong Kong Polytechnic University, Hong Kong, China

7c. Shandong Provincial Architectural Design Institute, Jinan, China

8

9 Phone: 0086 0531-86361236. Fax: 0086 0531-86361236.

10 Email: wenkezhang2006@163.com

11 * Corresponding author

12

13**Abstract** Groundwater seepage can improve the heat transfer performance of borehole ground heat
14exchanger (BGHE), and the corresponding velocity is the significant parameter which shows the
15degree of seepage role. The paper presents the mathematical model while groundwater flows
16through BGHE, and the comparisons between pure conduction and the combined heat transfer
17including conduction and convection are made. Points are set around borehole to test the
18temperature response at different time and then the goal functions containing both model results and
19test results are established. Next, the back calculation method is employed to obtain the value and
20orientation of velocity and therefore the convection role can be expressed. The reasonable points'
21locations along both depth and radial directions are analyzed; the comparisons of points'
22temperature responses are made according to the variation of seepage orientation and value. The
23relativity between points' locations and velocity value is discussed to make the calculation result
24acceptable. In addition, a number of trials are made to check the validity of back calculation
25method. The temperature response curves of points are shown and the characteristics embodied are
26investigated. Accordingly, the finite line heat source seepage model is significant to realize
27groundwater velocity.

28

29**Keywords:** groundwater seepage; borehole ground heat exchanger; velocity; finite line heat source;
30back calculation; partial derivative.

Nomenclature		
k	thermal conductivity ($\text{W m}^{-1} \text{K}^{-1}$)	<i>Superscript</i>
m	substitute variable	\int integration parameter
F	sum of squared deviation	Δ the first order derivative
a	thermal diffusivity ($\text{m}^2 \text{s}^{-1}$)	<i>Subscripts</i>
c_p	specific heat ($\text{J kg}^{-1} \text{K}^{-1}$)	i infinite line heat source
t_0	initial temperature (K)	f finite line heat source
t	temperature (K)	exp experiment
r	distance between point and borehole center (m)	cal calculation
Fo	Fourier number	<i>Greek symbols</i>
u	value of groundwater velocity (m/s)	β angular coordinate of points
U	dimensionless value of groundwater velocity	τ time (s)
x, y, z	rectangular coordinate (m)	φ orientation of groundwater velocity
X, Y, Z	dimensionless rectangular coordinate	Θ dimensionless excess temperature
h	depth of borehole	θ excess temperature (K)
H	dimensionless depth of borehole	
q_l	heating rate per meter line heat source (W m^{-1})	

31

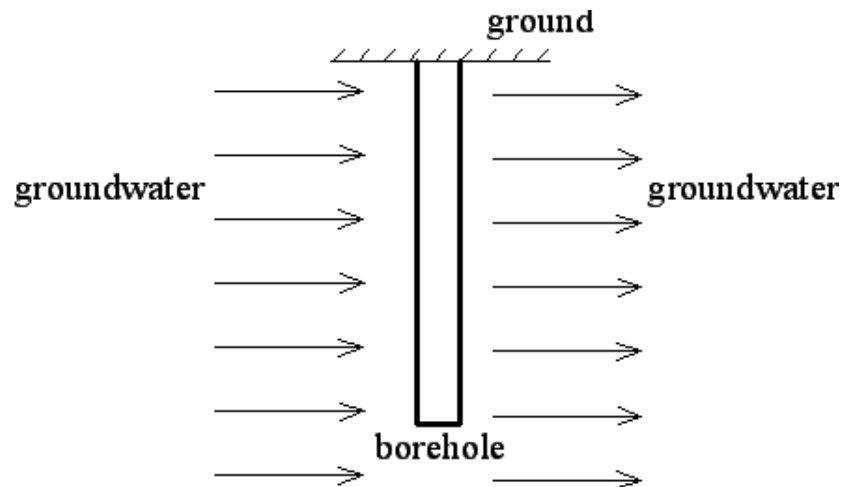
32

331. Introduction

34

35 The groundwater seepage often exists in underground medium and therefore groundwater can
36 flow through borehole ground heat exchanger (BGHE) while ground source heat pump (GSHP)
37 system is employed. The heat transfer mode is converted from pure conduction to combined style
38 including conduction and advection [1]. It is generally appreciated that the performance of the
39 GSHP system is greatly determined by the heat transfer ability of BGHE, this is because the heat is
40 released to underground in summer and extracted from underground in winter. However, it is
41 difficult to obtain the accurate velocity of groundwater as the underground composition is complex,
42 and most of the time groundwater effect is always ignored. Consequently, the traditional conduction
43 calculation is still the main mode in terms of designing size of BGHE. There is a belief that the
44 moving of groundwater is favorable to improve heat transfer performance, because groundwater
45 advection makes the heat accumulation around BGHE alleviated and therefore the thermal
46 transmission from BGHE to the surrounding becomes easier [2]. The design size of BGHE can be
47 saved provided that the groundwater seepage is taken into account, the initial cost spent on drilling
48 boreholes and installing thermal exchange tubes can be reduced, which means the economic
49 efficiency is improved and this will promote the application and development of GSHP technology
50 [3]. The diagram about groundwater seepage is shown in Fig.1 showing that groundwater flows

51through BGHE as a result of hydraulic gradient [4]. The velocity value and orientation are both
52determined by the local hydraulic gradient, the larger the gradient, the intenser the seepage.



53
54

Fig.1 The schematic diagram of groundwater which flows past BGHE

55 The order magnitude of velocity value is always minor and thus it is not easy to comprehend the
56value and orientation of velocity [5], the groundwater velocity is determined by the local hydraulic
57gradient [6]. As a result, the calculation results of heat transfer are unsatisfactory even though the
58existing model is employed. Attempts have been made to develop back calculation depending on
59the infinite line heat source model with groundwater seepage and both the value and orientation can
60be acquired. The difference between infinite and finite model is whether the depth of BGHE is
61considered. The infinite model only takes two-dimensional heat transfer into account but the depth
62of any BGHE is finite rather than infinite; the calculation result of the infinite model is not accurate
63due to the discrepancy with actual BGHE length. The impact of ground boundary should be
64considered once the finite model is applied not only for pure conduction but also for combined heat
65transfer [7-9], the finite model is in possession of distinctive characteristics compared with the
66infinite case. Given that the velocity is obtained with the help of back calculation based on the finite
67line heat source seepage model, the result is more reasonable than that acquired from infinite case.

68 The underground temperature response shows different states while the value and orientation of
69groundwater velocity differ. Therefore, the calculation at relevant positions can be carried out to lay
70a firm foundation for back calculation. The analysis on groundwater seepage is significant because
71it can demonstrate the advection role of groundwater. The heat transfer from BGHE to the
72surrounding underground medium includes conduction through its solid matrix and liquid (water) in
73its pores as well as by convection of the moving groundwater. In addition, the detailed researches
74are conducted to understand groundwater velocity. The design size of BGHE can be reduced if the

75velocity is recognized, which means the economic performance will be improved. The finite line
 76heat source seepage model is significant to achieve the groundwater velocity.

772. The mathematical model and corresponding analysis

78 2.1 The finite line heat source seepage model

79 The BGHE can be regarded as a line heat source because the ratio of length to radius is obviously
 80large; its depth is usually between 50m and 150m, and the radius is often from 130mm to 150mm. It
 81is evident that the radius is very small compared with the length and therefore the line heat source is
 82feasible [10, 11], and the line source emits heat from the time τ' with the heat transfer intensity q_l .
 83When groundwater passes BGHE, if line source is regarded as immovable then the groundwater is
 84movable.

85 In general, the hydraulic gradient is also two-dimensional within a certain depth of strata though
 86sometimes three-dimensional seepage exists; the two-dimensional flow is recommended as the
 87precondition to simplify the difficulty of investigation. On condition that the line heat source locates
 88at z -axis and emits heat from the time τ' while groundwater flows through it, the underground
 89temperature response at any point except heat source at the time τ can be shown while the ground
 90boundary effect is ignored, the corresponding formula is shown in Equation (1).

$$91 \quad \theta_i = \frac{q_l}{4\pi k} \int_0^{\tau} d\tau' \frac{1}{(\tau - \tau')} \exp \left[-\frac{[x - u \cos \varphi(\tau - \tau')]^2 + [y - u \sin \varphi(\tau - \tau')]^2}{4a(\tau - \tau')} \right] d\tau' \quad (1)$$

92 where u and φ are respectively the value and the orientation of groundwater velocity, orientation is
 93the intersection angle from the positive x axis to the direction of seepage, thus the parameter φ is
 94used to depict the this parameter. $\theta_i = t - t_0$, t and t_0 are respectively transient temperature and initial
 95temperature of any underground point except heat source, a is the thermal diffusivity of
 96underground medium. However, the depth of actual BGHE is finite and the infinite model cannot
 97embody the accurate heat transfer process; the existence of ground boundary should be emphasized
 98and thereby the finite line heat source model is suggested to establish a mathematical model
 99presenting both conduction and advection, and the detailed information is demonstrated in Equation
 100(2).

101

$$\left\{ \begin{array}{l}
\frac{\partial \theta}{\partial \tau} + u \cos \varphi \frac{\partial \theta}{\partial x} + u \sin \varphi \frac{\partial \theta}{\partial y} = a \left(\frac{\partial^2 \theta}{\partial x^2} + \frac{\partial^2 \theta}{\partial y^2} + \frac{\partial^2 \theta}{\partial z^2} \right) \\
\text{for } -\infty < x < +\infty, -\infty < y < +\infty, 0 \leq z < +\infty \\
\tau = \tau', t = t_0 \\
\tau > \tau', \sqrt{x^2 + y^2} \rightarrow \infty : t = t_0 \\
\tau > \tau', \sqrt{x^2 + y^2} \rightarrow 0 : \pi k \frac{\partial \theta}{\partial \sqrt{x^2 + y^2}} 2 \sqrt{x^2 + y^2} = q_l \\
\tau \geq \tau', z = 0 : t = t_0
\end{array} \right. \quad (2)$$

102 The boundary temperature is constant during the whole thermal exchange period [12], BGHE
103 extends from the boundary to the certain depth location below ground, the initial coordinate and the
104 termination coordinate of z for BGHE are respectively 0 and h , in such a way the analysis procedure
105 can be relatively convenient. The problem of convection can be considered either as cases in which
106 heat sources move through a fixed groundwater, or as cases of heat production with fixed sources
107 past which the groundwater flows. The BGHE is regarded as motionless while groundwater flows
108 in x - and y -direction, and the corresponding velocity along two directions are u_x and u_y respectively.
109 Based on Equation (2), define the motionless coordinates as (x, y, z) and the coordinates moving
110 together with the medium as (ξ, η, ζ) . The conversion between the two coordinate systems are $x = \xi$
111 + $u_x \tau$, $y = \eta + u_y \tau$, $z = \zeta$. The heat conduction caused by moving medium can be solved by Green
112 function, that is, by way of integration of the solutions for instantaneous point source. If an amount
113 of heat ρc is released at the point (x', y', z') at time τ' , the point (ξ, η, ζ) of the moving medium at
114 time τ , was at $[x - u_x(\tau - \tau'), y - u_y(\tau - \tau'), z]$ at time τ . The velocity along x - and y -direction can be
115 expressed as $u_x = u \cos \varphi$ and $u_y = u \sin \varphi$. Afterwards, the temperature response to the instantaneous
116 point source emitted at (x', y', z') at τ' is the Green function under the condition of groundwater
117 convection, and it can be written in Equation(3).

118

$$M(x, y, z, \tau; x', y', z', \tau') = \frac{1}{8 \sqrt[3]{a(\tau - \tau')}} \exp \left\{ - \frac{[x - x' - u \cos \varphi (\tau - \tau')]^2 + [y - y' - u \sin \varphi (\tau - \tau')]^2 + (z - z')^2}{4a(\tau - \tau')} \right\} \quad (3)$$

119 Accordingly, the temperature response of the finite heat source model while groundwater seepage
120 exists can be obtained by means of integration of Green function, and the corresponding expression
121 is displayed as follows.

122

$$\theta_f = \frac{q_l}{\rho c} \int_0^\tau \int_0^h M dz' d\tau' = \frac{q_l}{8\pi k} \int_0^\tau \frac{d\tau'}{\tau - \tau'} \times \exp \left[\frac{[x - u \cos \varphi(\tau - \tau')]^2 + [y - u \sin \varphi(\tau - \tau')]^2}{a(\tau - \tau')} \right] \times \left\{ \operatorname{erfc} \left[\frac{z-h}{2\sqrt{a(\tau - \tau')}} \right] - \operatorname{erfc} \left[\frac{z-0}{2\sqrt{a(\tau - \tau')}} \right] - \operatorname{erfc} \left[\frac{z+0}{2\sqrt{a(\tau - \tau')}} \right] + \operatorname{erfc} \left[\frac{z+h}{2\sqrt{a(\tau - \tau')}} \right] \right\} \quad (4)$$

123 Equation (4) which a number of parameters are involved in is complex . To simplify the form the
124 non-dimensional parameters are introduced.

125 $\Theta_f = k\theta_f/q_l$, $X = x/h$, $Y = y/h$, $U = uh/a$, $Fo = a\tau/h^2$, $Z = z/h$.

126 The dimensionless expression of Equation (4) is listed in Equation (5):

127

$$\Theta_f = \frac{1}{8\pi} \int_0^{Fo} \frac{dFo'}{Fo - Fo'} \times \exp \left[\frac{[X - U \cos \varphi(Fo - Fo')]^2 + [Y - U \sin \varphi(Fo - Fo')]^2}{4(Fo - Fo')} \right] \times \left\{ \operatorname{erfc} \left[\frac{Z-1}{2\sqrt{Fo - Fo'}} \right] - 2 \operatorname{erfc} \left[\frac{Z}{2\sqrt{Fo - Fo'}} \right] + \operatorname{erfc} \left[\frac{Z+1}{2\sqrt{Fo - Fo'}} \right] \right\} \quad (5)$$

128 Equation (5) clearly reveals the temperature response of the finite line heat source model with
129 groundwater seepage, which can be tilted as the finite line heat source seepage model. The seepage
130 role and ground boundary role are both reflected, accordingly the finite model is a significant
131 progress because it can improve the accuracy of calculation.

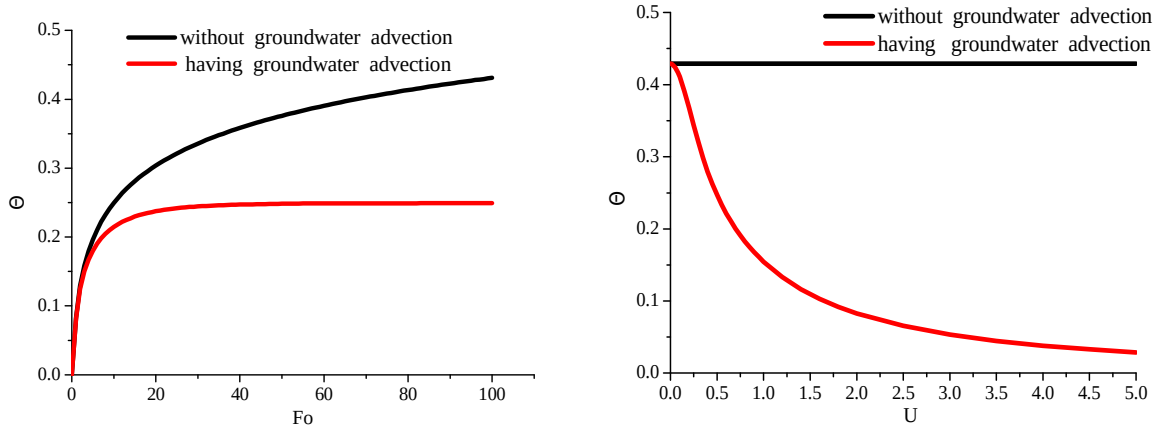
132

133 2.2 The difference between having groundwater seepage and without

134

135 When there is no groundwater seepage, the heat is emitted from the BGHE to the surrounding;
136 then the thermal response increases gradually until a stable state as a result of constant temperature
137 of ground boundary [13,14]; conduction is the only mechanism achieving heat transmission.
138 Groundwater flows through BGHE and then takes away a certain ratio of heat accumulated around
139 BGHE, the temperature difference between heat source and the surrounding increases to motivate
140 thermal transmission, and that thermal response degree is weaker than that induced by pure
141 conduction. It is beyond question that the relief level to heat accumulation which seepage give rise
142 to depends on seepage intensity i.e. velocity value U . With the increase of U , the contribution of
143 advection to the whole heat transfer process becomes increasingly outstanding [15,16]; this will
144 inevitably result in smaller and smaller temperature response. The two kinds of variation curves are
145 both illustrated in Fig.2, the temperature responses of seepage model adopted are the mean

146 responses. For one thing, pure conduction leads to larger response compared with combined heat
 147 transfer from the beginning to the end under the condition of constant velocity value U , this can
 148 prove that the seepage phenomenon is indeed favorable to improve heat transfer performance of
 149 BGHE. For another, if the time maintains unchanged, there is no velocity at all for pure conduction
 150 so that the temperature response holds a fixed value all the time, but the groundwater advection
 151 involved in combined heat transfer can let the response drop with the raised seepage strength [17].



152
 153

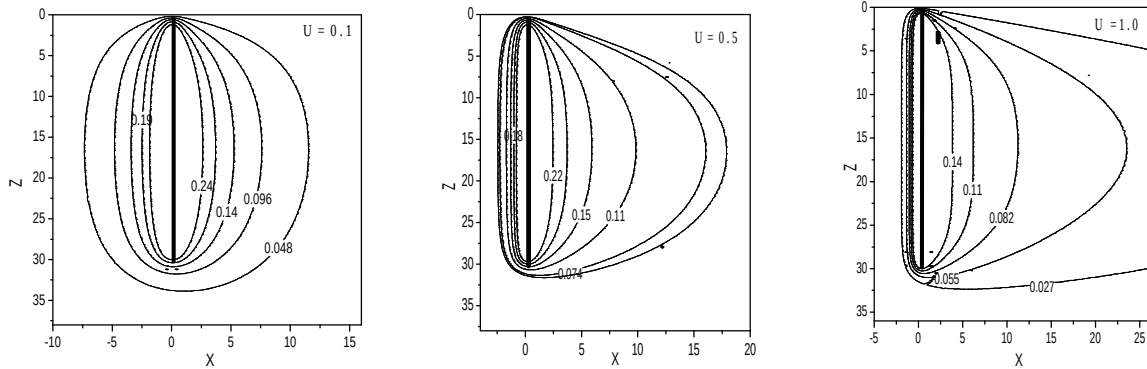
Fig.2 The comparison between pure conduction and combined heat transfer

154

155 2.3 The temperature field around BGHE

156

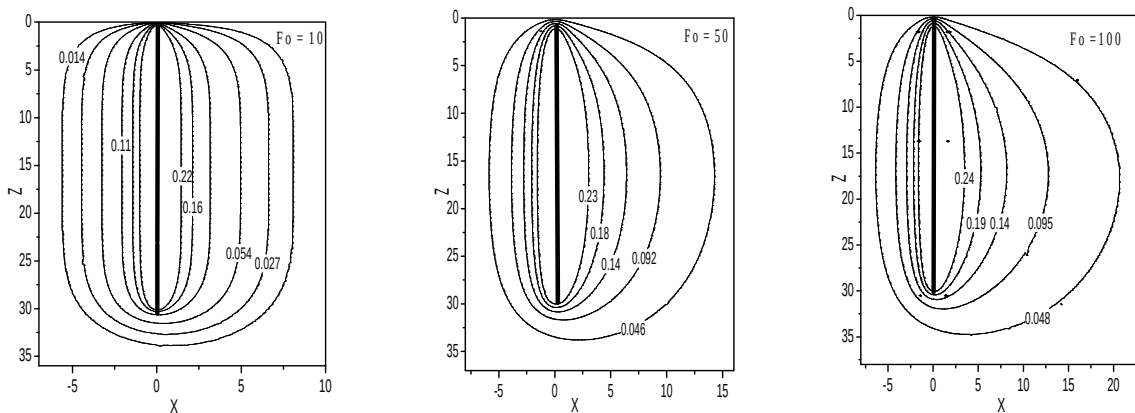
157 According to the analysis in section 2.2, the changes in terms of time and seepage intensity can
 158 bring about different thermal responses. BGHE is regarded as a line heat source with the constant
 159 heating rate q_l ; the surrounding underground medium presents changing temperature distributions
 160 with the velocity value or the time when groundwater passes BGHE. To exhibit the temperature
 161 distribution, the isothermals are shown while the seepage angle is 0° , which means at this time
 162 groundwater flows along positive direction of X -axis and some isothermals can be revealed while
 163 Fo and U respectively changes. Firstly, the temperature field varies with velocity values if a certain
 164 value is given to Fo , the isothermals are shown in Fig.3.



165
166

Fig.3 The isotherms with the increase of U

167 There shows delicate asymmetry of temperature distribution on both sides of Z -axis while U
 168 adopts minor value, because it seems that only pure conduction plays role in the heat exchange
 169 process. But if U attains a certain value, then the seepage effect is obvious. Isotherms depict the
 170 advection role and the temperature asymmetry is gradually notable; Fig.4 shows that temperature
 171 response on both sides of Z -axis presents different distribution with the time in the premise of
 172 constant U , which means the seepage effect is reflected by degrees.



173
174

Fig.4 The isotherms with the increase of Fo

175

1762.4 How the seepage orientation influences mean temperature response of BGHE

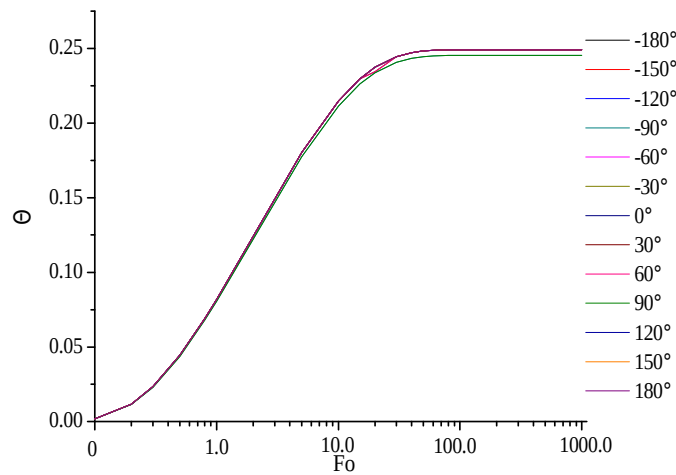
177

178 It is indisputable that the hydraulic gradient direction differs in different regions or areas; the
 179 seepage orientation exerts influence on the underground temperature field. The intersection angle
 180 between positive x -axis and seepage direction is from -180° to 180° . If the value of groundwater

181velocity is fixed i.e. the seepage intensity is unchangeable, different seepage directions lead to
 182temperature variation of any underground point [18]. However, from the perspective of mean
 183temperature response, the calculation findings are nearly the same. Equation (5) is the analytical
 184solution of temperature response at any point except heat source. Considering that the orientation of
 185seepage is two-dimensional, the integral average method can be utilized to acquire the mean
 186temperature response. Another integral is added to Equation (5) and the corresponding expression is
 187shown in Equation (6) which is a double integral.

$$\Theta_{ave,f} = \frac{1}{8\pi^2} \times \frac{1}{2\pi} \int_{-\pi}^{\pi} \int_0^{Fo} \frac{d\beta dFo'}{Fo - Fo'} \exp \left[\frac{[R \cos \beta - U \cos \varphi (Fo - Fo')]^2 + [R \sin \beta - U \sin \varphi (Fo - Fo')]^2}{4(Fo - Fo')} \right] \left\{ \operatorname{erfc} \left[\frac{Z - H}{2\sqrt{Fo - Fo'}} \right] - 2 * \operatorname{erfc} \left[\frac{Z}{2\sqrt{Fo - Fo'}} \right] + \operatorname{erfc} \left[\frac{Z + H}{2\sqrt{Fo - Fo'}} \right] \right\} \quad (6)$$

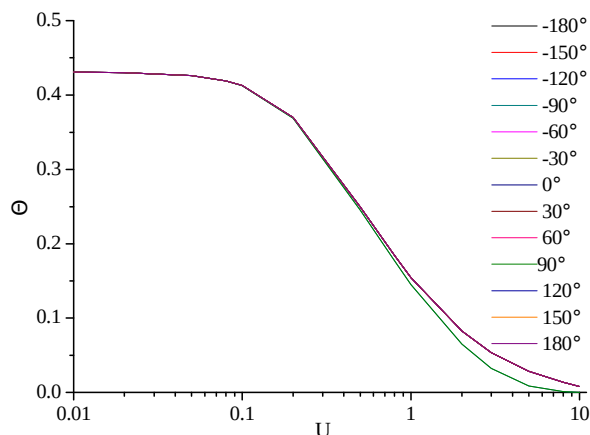
189 During the selection of intersection angles, some typical angles are chosen to discuss whether the
 190variation of groundwater seepage can induce the change of mean temperature response surrounding
 191BGHE. When assessing the improvement effect that groundwater seepage produces, it is significant
 192to calculate the mean temperature response rather than the response of one location or several
 193locations. We can obtain the mean temperature response trend of the external surface of BGHE with
 194the time and the circumstance is unfolded in Fig.5, and the value of groundwater velocity is
 195constant. Many angles including both negative and positive cases explain that the variation of
 196angles exerts a little impact on the mean temperature response of BGHE.



197
 198

Fig.5 The mean temperature response with the time when φ adopts different angles

199 Another trend is the variation curve of the mean temperature response with the increase of seepage
 200 intensity. Fig.6 shows that no matter what degree the velocity intensity is, the mean temperature
 201 responses of different seepage orientations are almost equal with each other while parameter U is
 202 the same.



203
 204 **Fig.6 The mean temperature response with the velocity value when ϕ adopts different angles**

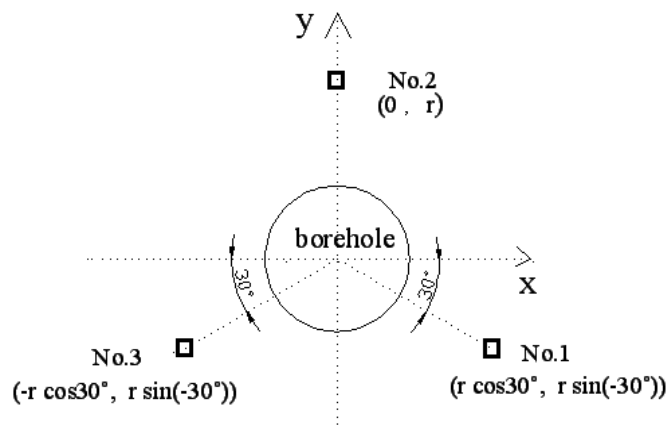
2053. The back calculation for groundwater velocity

206
 207 The role of groundwater seepage mainly depends on its velocity, but from what has been stated in
 208 section 1, the difficulty in obtaining the value and orientation of velocity is a remarkable problem
 209 that engineers and scholars have to deal with. The back calculation for groundwater velocity needs
 210 to be investigated; though the infinite line heat source seepage model is simpler than the finite case,
 211 BGHE has finite depth so that the finite line heat source seepage model is more suitable for the
 212 mathematical calculation. It is worthwhile to conduct the back calculation method based on the
 213 finite line heat source seepage model. The following paragraphs expound the fundamental
 214 principles of back calculation and corresponding characteristics.

2153.1 The applied measures before back calculation

216 The BGHE emits heat along different radial directions [19, 20], thus the temperature response of
 217 any point with the same radius to the center of BGHE should be equal with each other if there is no
 218 groundwater seepage, because the pure conduction executes with the same degree at every radial
 219 direction. At a certain depth, if some points with the same radius around BGHE are chosen, the
 220 temperature responses of these points will be different under the influence of groundwater seepage.
 221 Some thermal resistors are installed respectively at different points chosen. The accurate velocity is

222not known at first but the range is set in advance, thereby the value U and orientation φ are put into
 223the finite line heat source seepage model in the process of back calculation,; the accurate value can
 224be predicted while the difference between the calculation result and test data reaches the minimum
 225or even equal. It should be admitted that the back calculation result is not accurate if only one point
 226is applied, but the ultimate velocity can be acquired while the number of points attain a certain
 227value, which means the temperature response of every point obtained by mathematical model
 228simultaneously achieve the nearest approximation of test data, accordingly the U and φ can be
 229estimated. We suggest that three points are distributed at first to verify the back calculation method;
 230these points with the same radius are well even-distributed around BGHE, that is, the intersection
 231angle between every two adjacent points are equal with each other, this intersection angle is 120° .
 232Fig.7 gives a sample of arranging three points.



233
 234 **Fig.7 The schematic diagram of three even-distributed points around BGHE**

235
 236 Fig.7 shows one mode distributing three points; there are different modes if three points are even-
 237distributed, such as some cases depicted in Fig.8.

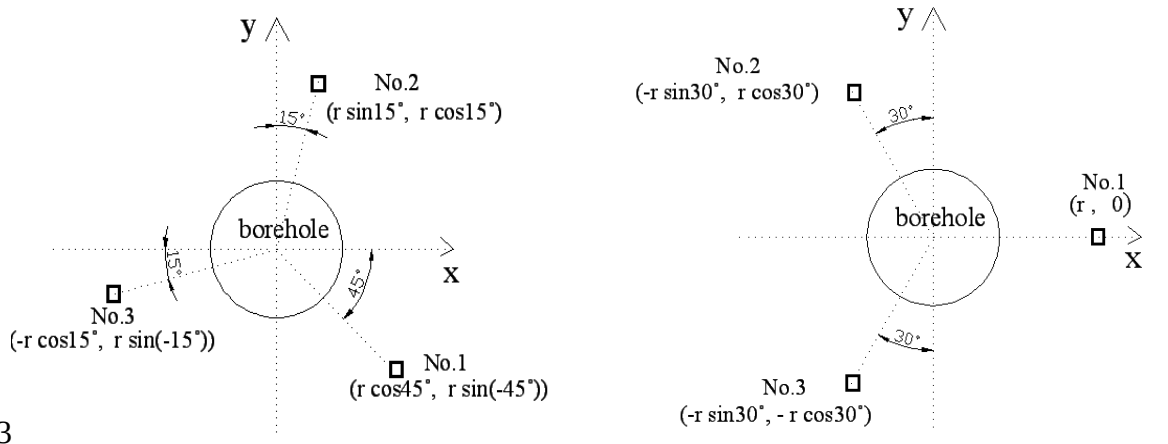
238

239

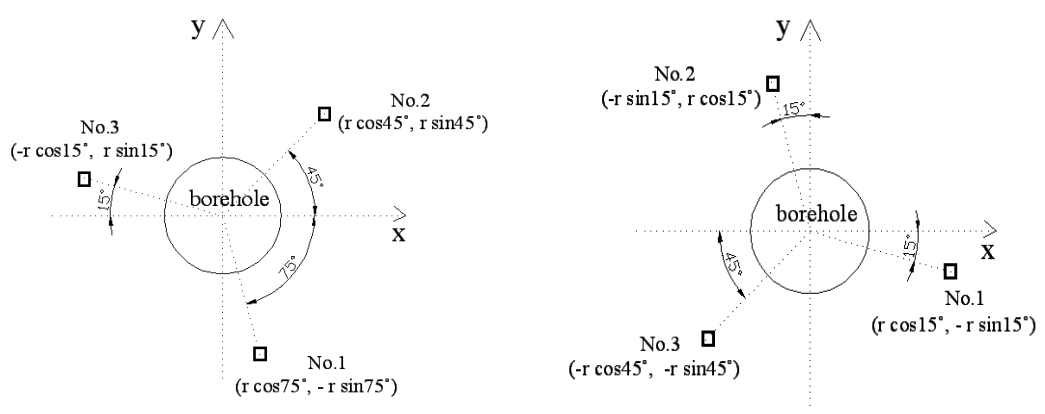
240

241

242



243



244

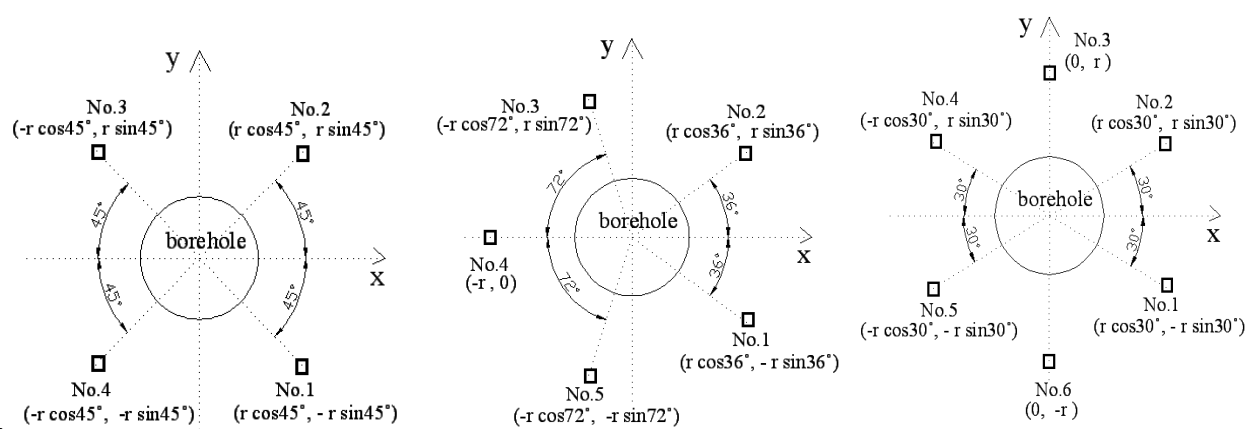
245

246

Fig.8 Some distributing modes for three points around BGHE

247

248 From the perspective of the number of points, the more the better, because added points can make
 249the accuracy of back calculation higher and higher, these points had better be arranged even-
 250distributed, four points, five points and six points are shown in Fig.9.



251

252

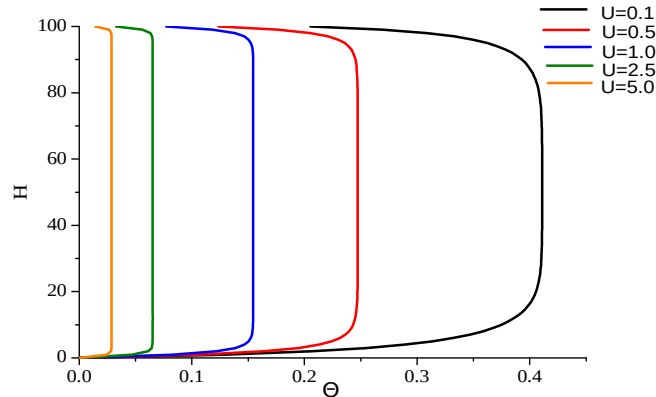
253

Fig.9 The distributing diagram while there are different number points

2543.2 The depth location of distributing points

255

256 As stated in section 3.1, the figures only describe the horizontal distributing information, now that
257the depth of any borehole is finite, how to select the depth location i.e. the value of Z is an
258important issue because this can determine the back calculation effect. The finite line heat source
259seepage model causes different temperature response degrees along Z -axis [21], and the temperature
260field on both sides of Z -axis are asymmetrical due to groundwater seepage [22,23]. The mean
261temperature response by means of Equation (5) can be calculated while Z picks different values
262along depth direction, and the corresponding thermal responses along Z -axis are listed in Fig.10
263while different values are assigned to U . It is clear that the temperature responses of the starting
264location area and final position area are weaker than other areas of depth direction; the middle area
265shows obviously stronger temperature responses. The horizontal plane while Z adopts the middle
266point of borehole depth can be selected to set three points.



267

268

Fig.10 The mean temperature response along Z -axis

269

2703.3 The relativity between points' radius to borehole center and velocity intensity

271

272 Though there are different options for selecting the number of points and the distributing modes,
273we still make full use of the case described in Fig.7 as the research basis of investigation. The
274middle depth location of borehole is decided to serve as the plane for distributing points, but how to
275determine the radius of point mainly rests with the seepage intensity. Three points are even-
276distributed no matter what the orientation is, and the difference must be generated in terms of
277temperature response. The next problem is to study the radius of point or the distance between
278points and the borehole center, because the radius should be adjusted according to the variation of
279 U . In view of this, the analytical solutions of temperature response of the finite line heat source

280 seepage model can be changed, if the radius from the point to the borehole center is r , the following
 281 non-dimensional parameters can be introduced.

282 $\Theta_f = k\theta_f/q_i$, $X = x/r$, $Y = y/r$, $U = ur/a$, $Fo = a\tau/r^2$, $H = h/r$, $Z = z/r$.

283 Because $x = r \cos \beta$ and $y = r \sin \beta$, β means the angular coordinate of points distributed around
 284 borehole. Afterwards the new dimensionless temperature response is obtained as follows:

285
$$\Theta_f = \frac{1}{8\pi} \int_0^{Fo} \frac{dFo'}{Fo - Fo'} \times \exp \left[\frac{[\cos \beta - U \cos \varphi(Fo - Fo')]^2 + [\sin \beta - U \sin \varphi(Fo - Fo')]^2}{4(Fo - Fo')} \right] ; \quad (7)$$

$$\left\{ \operatorname{erfc} \left[\frac{Z - H}{2\sqrt{Fo - Fo'}} \right] - 2 \operatorname{erfc} \left[\frac{Z}{2\sqrt{Fo - Fo'}} \right] + \operatorname{erfc} \left[\frac{Z + H}{2\sqrt{Fo - Fo'}} \right] \right\}$$

286 The non-dimensional parameter U consists of actual velocity value u , radius r of three points and
 287 thermal diffusivity a of underground medium, accordingly the parameter U can embody the
 288 relativity between u and r . Because r delegates the distance from those points to the borehole center,
 289 this distance should be adjusted to make the back calculation result satisfactory. Equation (7) is
 290 taken advantage of while Z adopts $H/2$ to calculate the temperature responses of three points. The
 291 range of seepage orientation is $[-180^\circ, 180^\circ]$, and a certain value from this range is chosen and then
 292 taken into Equation (7), the variation trend of temperature responses with U is expressed in Fig.11,
 293 it is clear that the response degrees decrease with the enhancement of seepage intensity U . Two
 294 factors should be considered for choosing the value of U , one factor is that the temperature response
 295 difference of three points should be clear as a result of U because notable difference is beneficial to
 296 carry out back calculation; another factor is that their temperature responses should not be too small
 297 because too small values are easy to result in calculation error.

298

299

300

301

302

303

304

305

306

307

308

309

310

311

312

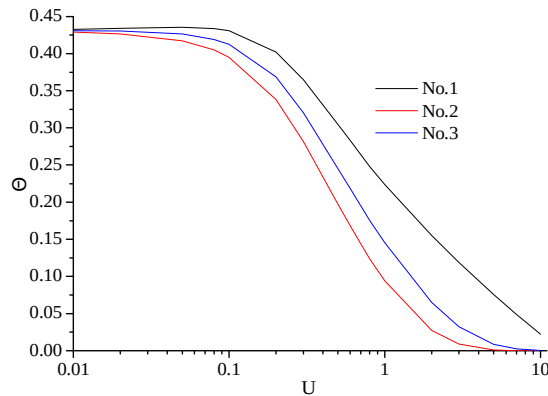


Fig.11 The temperature responses of three points with U

313

314 Based on the two factors the range of U should be [0.1, 5.0], which means the relativity between
315points' radius r to borehole center and actual velocity intensity u can be summarized, i.e. the
316product of u and r lies in the range [0.1 a , 5.0 a].

3173.4 The back calculation principles

318

319 The data of actual temperature t of three points can be recorded at regular time interval if these
320points have been set at suitable locations. Non-dimensional temperature response $\Theta_{f,exp}$ at different
321time is $k\theta_f/q_1$ i.e. $k(t - t_0)/q_1$, the initial temperature t_0 and the thermal conductivity of underground
322medium can be known by relevant test equipment, and the heat transfer quantity per meter BGHE q_1
323can be calculated based on relevant parameters which are obtained directly by test equipments. As
324stated above, although the accurate velocity of groundwater cannot be known at first, the range can
325be set for the value U and direction φ and the corresponding interval should be small enough.
326Afterwards U and φ are continually taken out from the corresponding range to be put into Equation
327(7), the parameters except U and φ are known at different time. The corresponding $\Theta_{f,cal}$ can be
328achieved after finishing calculation according to Equation (7). There are a number of data being
329recorded at regular time interval; meanwhile, the calculation result by means of model at regular
330time interval can be acquired. Therefore, there exists recorded data and the corresponding
331calculation data at the same time. When the comparisons are made between two different kinds of
332data, the difference between them at different time should be calculated altogether because the total
333difference of the whole process should be the basis of back calculation. If the total difference
334reaches the minimum, it can be concluded the corresponding U and φ are respectively the actual
335cases. For that reason a goal function F shown in Equation (8) is the sum of squared deviation from
336test result to calculation result.

337

$$F(U, \varphi) = \sum_{i=1}^n (\Theta_{f,cal} - \Theta_{f,exp})^2 \quad (8)$$

338 From the beginning to the end, the data are recorded and calculated with the time at regular
339interval. If F can achieve the minimal value, the actual U and φ can be determined [24,25].
340Equation (8) is a binary function with two independent variables U and φ . If the goal function F
341makes first order partial derivative respectively towards parameter U and φ , and the symbol F'_U and
342 F'_φ are the corresponding first order partial derivatives. When Eq.(8) arrives at the minimum, at that
343time the values of F'_U and F'_φ must be zero. Considering that both U and φ are discrete variables

344 rather than continuous variables, it cannot be guaranteed that the values of F'_U and F'_φ must be zero.
 345 But the minor values which is next to zero can be endowed respectively to F'_U and F'_φ , and the
 346 minor values can be adjusted according to the calculation process to limit U and φ to smaller and
 347 smaller range, the best finding is the single U and φ can be found at last.

348 Firstly, the formula of F'_U is demonstrated in Equation (9)

$$\begin{aligned}
 F'_U \Delta &= 2 \sum_{i=1}^n (\Theta_{f,cal} - \Theta_{f,exp}) \times \Theta'_{f,cal} = 2 \sum_{i=1}^n \left\{ \frac{1}{8\pi} \int_0^{F_{o_i}} \frac{1}{(F_{o_i} - F_{o'})} \exp \left[-\frac{[\cos \beta - U \cos \varphi (F_{o_i} - F_{o'})]^2 + [\sin \beta - U \sin \varphi (F_{o_i} - F_{o'})]^2}{4(F_{o_i} - F_{o'})} \right] \times \right. \\
 &\quad \left. \left\{ \operatorname{erfc} \left[\frac{Z-H}{2\sqrt{F_{o_i} - F_{o'}}} \right] - 2 * \operatorname{erfc} \left[\frac{Z}{2\sqrt{F_{o_i} - F_{o'}}} \right] + \operatorname{erfc} \left[\frac{Z+H}{2\sqrt{F_{o_i} - F_{o'}}} \right] \right\} dF_{o'} - \Theta_{f,exp} \right\} \\
 349 \quad &\times \frac{1}{8\pi} \int_0^{F_{o_i}} \frac{1}{(F_{o_i} - F_{o'})} \exp \left[-\frac{[\cos \beta - U \cos \varphi (F_{o_i} - F_{o'})]^2 + [\sin \beta - U \sin \varphi (F_{o_i} - F_{o'})]^2}{4(F_{o_i} - F_{o'})} \right] \times \\
 &\quad \left\{ \operatorname{erfc} \left[\frac{Z-H}{2\sqrt{F_{o_i} - F_{o'}}} \right] - 2 * \operatorname{erfc} \left[\frac{Z}{2\sqrt{F_{o_i} - F_{o'}}} \right] + \operatorname{erfc} \left[\frac{Z+H}{2\sqrt{F_{o_i} - F_{o'}}} \right] \right\} \times \\
 &\quad \frac{2 [\cos \beta - U \cos \varphi (F_{o_i} - F_{o'})] \cos \varphi (F_{o_i} - F_{o'}) + 2 [\sin \beta - U \sin \varphi (F_{o_i} - F_{o'})] \sin \varphi (F_{o_i} - F_{o'})}{4(F_{o_i} - F_{o'})} dF_{o'}
 \end{aligned} \tag{9}$$

350

351 Secondly the detailed information on F'_φ is illustrated in Eq.(10).

$$\begin{aligned}
 F'_\varphi \Delta &= 2 \sum_{i=1}^n (\Theta_{f,cal} - \Theta_{f,exp}) \times \Theta'_{f,cal} = 2 \sum_{i=1}^n \left\{ \frac{1}{8\pi} \int_0^{F_{o_i}} \frac{1}{(F_{o_i} - F_{o'})} \exp \left[-\frac{[\cos \beta - U \cos \varphi (F_{o_i} - F_{o'})]^2 + [\sin \beta - U \sin \varphi (F_{o_i} - F_{o'})]^2}{4(F_{o_i} - F_{o'})} \right] \times \right. \\
 &\quad \left. \left\{ \operatorname{erfc} \left[\frac{Z-H}{2\sqrt{F_{o_i} - F_{o'}}} \right] - 2 * \operatorname{erfc} \left[\frac{Z}{2\sqrt{F_{o_i} - F_{o'}}} \right] + \operatorname{erfc} \left[\frac{Z+H}{2\sqrt{F_{o_i} - F_{o'}}} \right] \right\} dF_{o'} - \Theta_{f,exp} \right\} \\
 352 \quad &\times \frac{1}{8\pi} \int_0^{F_{o_i}} \frac{1}{(F_{o_i} - F_{o'})} \exp \left[-\frac{[X - U \cos \varphi (F_{o_i} - F_{o'})]^2 + [Y - U \sin \varphi (F_{o_i} - F_{o'})]^2}{4(F_{o_i} - F_{o'})} \right] \times \\
 &\quad \left\{ \operatorname{erfc} \left[\frac{Z-H}{2\sqrt{F_{o_i} - F_{o'}}} \right] - 2 * \operatorname{erfc} \left[\frac{Z}{2\sqrt{F_{o_i} - F_{o'}}} \right] + \operatorname{erfc} \left[\frac{Z+H}{2\sqrt{F_{o_i} - F_{o'}}} \right] \right\} \times \\
 &\quad \frac{-2 [\cos \beta - U \cos \varphi (F_{o_i} - F_{o'})] \times U \sin \varphi (F_{o_i} - F_{o'}) + 2 [\sin \beta - U \sin \varphi (F_{o_i} - F_{o'})] \times \cos \varphi (F_{o_i} - F_{o'})}{4(F_{o_i} - F_{o'})} dF_{o'}
 \end{aligned} \tag{10}$$

353

354 As there are three points and therefore three goal functions need to be established. Only one goal
 355 function may not determine the accurate velocity, but three goal functions are highly possible to

356determine the velocity. For every goal function, the values of F'_U and F'_φ are respectively zero or
 357minor values, which means two limitations are set for every function to let function reach the
 358minimum. Accordingly, there are six conditions while three functions simultaneously reach the
 359minimum. There are many conditions so that velocity can be limited to a single case, and this is the
 360reason of setting three points rather than only one point. But if the accurate velocity cannot be
 361found in such a way, there are some or a small range of velocities meeting the six conditions, these
 362remaining velocities will be put into Equation (8) one by one for comparing different results, then
 363the single velocity can be discovered because this velocity let the result of Equation (8) reach the
 364minimum.

365

3664. The relevant characteristics and trials of back calculation

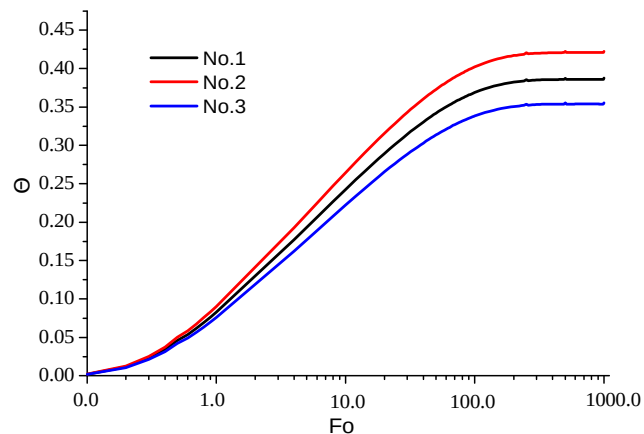
367

3684.1 The influence that orientation exerts on the comparisons of three points

369

370 The locations of three points have been fixed as shown in Fig.7. The temperature responses of
 371points will raise with the time when U and φ are given confirmed values, and the relative size with
 372each other is explicit. One example of specific U and φ is shown in Fig.12, and the orientation of
 373groundwater flow is 60° .

374



375

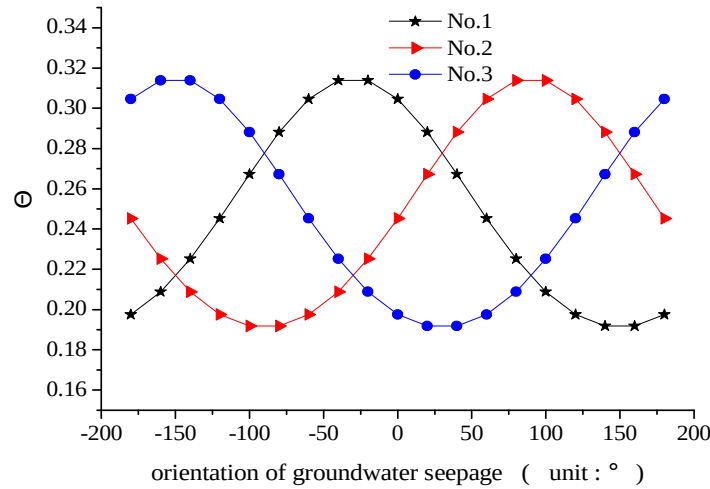
376

Fig.12 The temperature responses of three points with the time

377 Seepage role is an incitement of impacting temperature responses of points, and the influence
 378degrees rest with the velocity [26]. All these temperature responses decrease with the increase of
 379velocity intensity U , but when it comes to comparisons made for three temperature responses, the
 380seepage orientation indeed plays a vital role. With the variation of orientation, the temperature

381 response of every point shows fluctuation ceaselessly if the time and velocity intensity are constant,
 382 it means that the relative size in comparison to each other varies with the adjustment of orientation,
 383 the detailed information is observed in Fig.13.

384



385
 386

Fig.13 The temperature responses of three points with the change of orientation

387

388 4.2 The change trend of slope of temperature responses

389

390 The curves shown in Fig.12 indicate that the whole trend of temperature response is ever-
 391 increasing until a stable state. In the process of temperature increase, firstly those curves go through
 392 the stage that slopes keep continuous growth, next there is a period when slopes decrease, and at
 393 last all the curves will arrive at stable states. Equation (7) is the analytical solution of any point
 394 except heat source, thereby the slope of temperature response to time can be listed by means of the
 395 first order derivative of Θ to F_0 . The substitute variable m is used and $m = F_0 - F_0'$ so that
 396 Equation (7) is transformed into Equation (11).

397

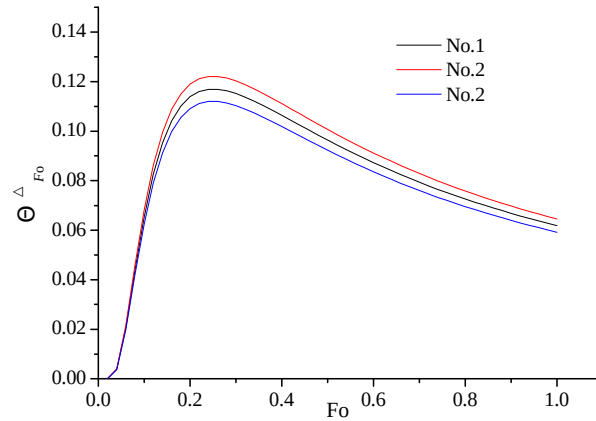
$$\Theta_f = \frac{1}{8\pi} \int_0^{F_0} \frac{dm}{m} \times \exp \left[\frac{(\cos \beta - Um \cos \varphi)^2 + (\sin \beta - Um \sin \varphi)^2}{4m} \right] \times \left\{ \operatorname{erfc} \left[\frac{Z-H}{2\sqrt{F_0-F_0'}} \right] - 2\operatorname{erfc} \left[\frac{Z}{2\sqrt{F_0-F_0'}} \right] + \operatorname{erfc} \left[\frac{Z+H}{2\sqrt{F_0-F_0'}} \right] \right\} \quad (11)$$

398 And the first order derivative of Θ to F_0 can be gained in Equation (12).

399

$$\Theta_{Fo}^{\Delta} = \frac{1}{8\pi} \times \frac{1}{Fo} \exp \left[\frac{(\cos \beta - U \times Fo \cos \varphi)^2 + (\sin \beta - U \times Fo \sin \varphi)^2}{4Fo} \right] \left\{ \operatorname{erfc} \left[\frac{Z-H}{2\sqrt{Fo-Fo'}} \right] - 2 \operatorname{erfc} \left[\frac{Z}{2\sqrt{Fo-Fo'}} \right] + \operatorname{erfc} \left[\frac{Z+H}{2\sqrt{Fo-Fo'}} \right] \right\} \quad (12)$$

400 For three points, the change trends of slopes with the time are displayed in Fig.14 while U and φ
 401 remain changeless.



402

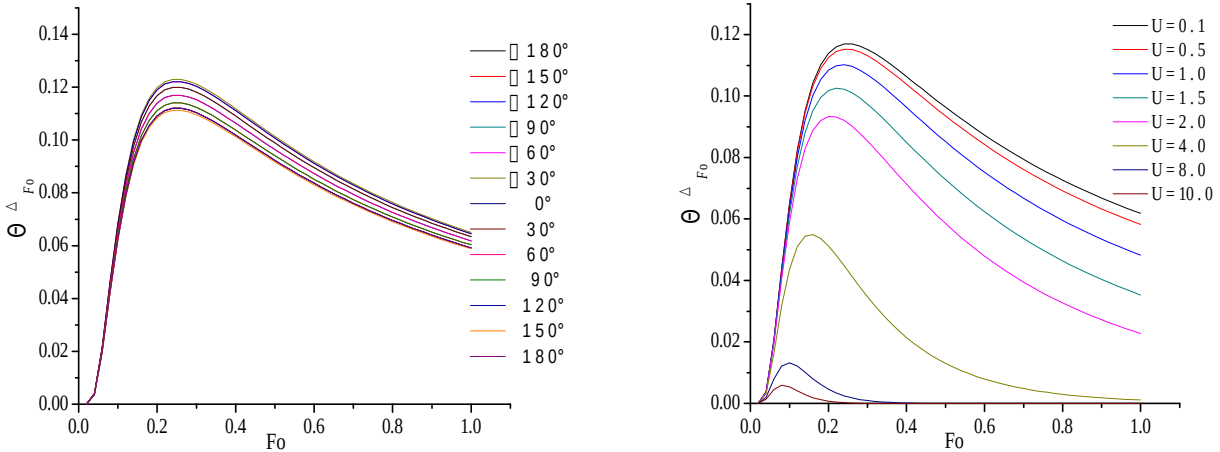
403

Fig.14 The variation trend of slopes of three pints while U and φ remain changeless

404

405 It can be found that the time when the slopes stop rising trend and begin to decrease are nearly the
 406 same for three points. From another perspective, because change trends of slopes of all points
 407 present the same regular pattern and the corresponding time is nearly equal. Consequently one point
 408 can be chosen to explore the slope trend under the conditions of different seepage directions, at that
 409 time the seepage intensity U is invariable. Meanwhile, the influence which velocity intensity exerts
 410 on the slope trend of one point can be studied if the seepage orientation is fixed. Fig.15 can depict
 411 corresponding conclusions with reference to these problems.

412



413
 414 **Fig.15 The variation trend of slope when orientation and velocity intensity varies respectively**

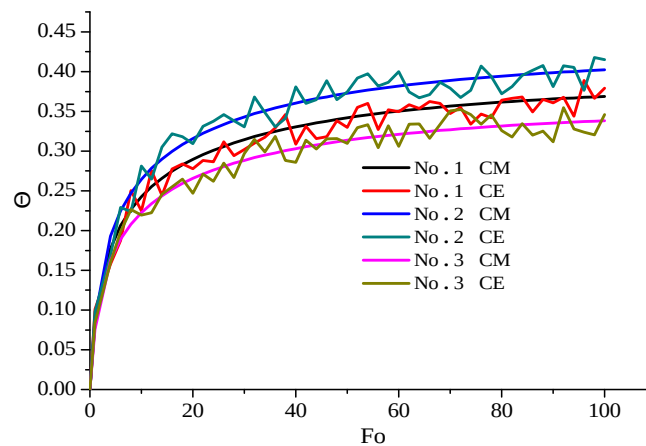
415 The curves shown in Fig.15 explain that change of orientation can slightly alter the extent of
 416 slope but has no impact on the whole regular pattern even route, especially for the time point at
 417 which slope turns from increase to decrease, this time point does not change with the variation of
 418 orientation. In addition, the strengthening of U can affect the slope curves not only the extent but
 419 also the route. The slope extent drops with the enhancement of velocity value, and the time when
 420 the transformation between rise and fall occurred becomes shorter and shorter.

421 4.3 The back calculation trials

422

423 The principles of back calculation for obtaining velocity of groundwater are summarized above.
 424 Next, the actual experimental data and the theoretical results will be employed to check the
 425 rationality of back calculation. Three points are distributed around BGHE to record the
 426 experimental data at regular time interval. The range of U is known according to the local
 427 underground hydraulic data and the range of φ is $[-180^\circ, 180^\circ]$. The experimental data of
 428 temperature response with the time can be recorded and the corresponding non-dimensional
 429 temperature response can be obtained. The range of U and φ are set and then the iterations for them
 430 are conducted, which means U and φ are continuously picked from their ranges and then the values
 431 are put into Equation (7) to obtain the non-dimensional temperature response of theoretical model.
 432 Thus, the temperature response curves of three points can be obtained by theoretical calculation.
 433 Commonly the recorded data curves fluctuate and have obvious deviation with the model curves.
 434 By means of back calculation method, the accurate values of U and φ can be determined while the
 435 goal function achieves the minimum. The relevant signs CM and CE are respectively the calculation

436result of model and the experiment data. The theoretical model circumstances and experimental
 437circumstances of three points are illustrated in Fig.16. Some examples were selected in the process
 438of trials, for example, when U and φ respectively adopts 0.2 and 60° , theoretical result of the model
 439can be obtained and the experimental data are recorded. Having used the back calculation based on
 440the principles introduced above, the velocity intensity U and orientation φ can be found. In addition,
 441other examples were tried to verify the back calculation, and the effect can shows that the back
 442calculation method is reasonable of obtaining groundwater velocity.



443
 444

Fig.16 The temperature responses of both model calculation and experiments

4455. Conclusions

446

447 With the development of GSHP technology, the research on groundwater seepage is becoming
 448increasingly important, this is due to the fact that the advection of groundwater can improve the
 449heat transfer ability of BGHE so that the performance of the whole system can be ameliorated. The
 450paper analyzes the relevant characteristics involved in the heat exchanger process between BGHE
 451and surrounding underground medium while groundwater flows though BGHE. The underground
 452temperature field is unavoidably affected by seepage role. By means of comparison between pure
 453conduction and combined heat transfer including conduction and groundwater advection, the
 454significance of investigating the groundwater seepage can be proven. It goes without saying the
 455most difficult task is to comprehend the groundwater velocity including value and orientation,
 456therefore the back calculation method based on the finite heat source seepage model is proposed.
 457Combined with the relevant knowledge of advanced mathematics, the goal function is established
 458for acquiring the velocity. The derivative is utilized according to the principles of how to achieve

459the extreme value of multivariable function. Some characteristics derived from back calculation are
460investigated to explain the essence of method in detail. The back calculation method provide
461convenience for obtaining the groundwater velocity because only the temperature response is
462enough to achieve the groundwater velocity; this method is valuable for investigating the influence
463that groundwater seepage exerts on heat transfer of BGHE. The content of this paper mainly
464propose a theoretical method based on the reasonable principles, which can provide theoretical
465guidance for obtaining groundwater velocity while actual experiment is done.

466

467 **Acknowledgement**

468

469The work described in this paper was supported by the grant PolyU 152039/15E from The Hong
470Kong Polytechnic University, and was partially supported by Natural Science Foundation of China
471(NSFC) No.51176104.

472

473

474 **References**

475

476[1] Nairen Diao, Qinyun Li, Zhaohong Fang. Heat transfer in ground heat exchangers with
477groundwater advection, *International Journal of Thermal Sciences* 43 (2004) 1203–1211.

478[2] Lin Yun, Further Study on Heat Transfer Model and Design of Geothermal Heat Exchangers,
479Master Thesis, Department of Thermal Engineering, Shandong Jianzhu University, 2010.

480[3] Chiasson A D, Ress S J, Spitelier J D. A preliminary assessment of the effects of groundwater
481flow on closed-loop ground-source heat pump systems, *ASHRAE Transactions* 106(1) (2000) 380-
482393.

483[4] Nairen Diao, Zhaohong Fang. *Ground-Coupled Heat Pump Technology*. 1st ed. Beijing: Higher
484Education Press, 2006.

485[5]Shi Liangsheng, Liao Weihong, Yang Jinzhong, Cai Shuying, The Conditional Simulation of
486Groundwater Flow, *Journal of Sichuan University (Engineering Science Edition)* 41(6) (2009) 41-
48750.

488[6] United States Environment Protection Agency. *BIO-SCREEN, Natural attenuation decision*
489support system, user's manual, National Risk Management Research Laboratory, 1996.

490[7] Zeng H Y. A Finite Line-source Model for Borehole in Geothermal Heat Exchangers, *Heat*
491Transfer-Asian Research 31(7) (2002) 558-567.

492[8] Massimo Cimmino, Michel Bernier, François Adams, A contribution towards the determination
493of g-functions using the finite line source, *Applied Thermal Engineering* 51 (2013) 401-412.

494[9] Yavuzturk C, Spitler J D, Rees S J. A transient two-dimensional finite volume model for
495simulation of vertical U-tube ground heat exchanger[J]. *Ashrae Transactions*, 1999:465-474.

496[10] Tatyana V. Bandos, Álvaro Monterob, Esther Fernández. Finite line-source model for
497borehole heat exchangers: effect of vertical temperature variations, *Geothermics* 38 (2009) 263-270.

498[11] Carslaw H S, Jeager J C. *Conduction of Heat in Solids*, 2th ed. Oxford Press, Oxford, 1959.□

499[12] S. Koohi-Fayegh, M.A. Rosen, An analytical approach to evaluating the effect of thermal
500interaction of geothermal heat exchangers on ground heat pump efficiency, *Energy Conversion and*
501*Management* 78 (2014) 184-192.

502[13] Zeng Heyi. A Model of Finite-length Linear Heat Source for the Vertical Embedded Pipe of a
503Ground-source Heat Pump, *Journal of Engineering for Thermal Energy and Power* 18(104) (2003)
504166-169.

505[14] Mostafa H.Sharqawy, HassanM.Badr, EsmailM.Mokheimer, Investigation of buoyancy effects
506on heat transfer between a vertical borehole heat exchanger and the ground, *Geothermics* 48 (2013)
50752-59.

508[15] Nelson Molina-Giraldo, Philipp Blum, Ke Zhu, etc. A moving finite line source model to
509simulate borehole heat exchangers with groundwater advection, *International Journal of Thermal*
510*Sciences* 50 (2011) 2506-2513.

511[16] Huajun Wang, Chengying Qi, Hongpu Du, Jihao Gu, Thermal performance of borehole heat
512exchanger under groundwater flow: A case study from Baoding, *Energy and Buildings* 41 (2009)
5131368-1373.

514[17] Wenke Zhang, Hongxing Yang, Lin Lu, Zhahong Fang, The analysis on solid cylindrical heat
515source model of foundation pile ground heat exchangers with groundwater flow, *Energy* 55
516(2013)417-425.

517[18] Jung Chan Choi , Joonsang Park, Seung Rae Lee, Numerical evaluation of the effects of
518groundwater flow on borehole heat exchanger arrays, *Renewable Energy* 52 (2013) 230-240.

519[19] Yi Man, Hongxing Yang, Nairen Diao, Junhong Liu, Zhaohong Fang, A new model and
520analytical solutions for borehole and pile ground heat exchangers, *International Journal of Heat and*
521*Mass Transfer* 53 (2010) 2593-2601.

- 522[20] Huajun Wang, Chengying Qi, Hongpu Du, Jihao Gu, Improved method and case study of
523thermal response test for borehole heat exchangers of ground source heat pump system, *Renewable*
524*Energy* 35 (2010) 727-733.
- 525[21] Sherif L.Abdelaziz, TolgaY.Ozudogru, etc, Multilayer finite line source model for vertical heat
526exchangers, *Geothermics* 51 (2014) 406-416.
- 527[22] Liu Hu, Jin Hua, Xing Shuyan, etc, Influence of Groundwater Seepage on GHE Temperature
528Field, *Water Resources and Power* 30(12) (2012) 117-119.
- 529[23] Fan Rui, Ma Zuiliang, Heat Transfer Analysis of Geothermal Heat Exchanger Under Coupled
530Conduction and Groundwater Advection. *Acta Energiae Solaris Sinica* 27(11) (2006) 1155-1162.
- 531[24] Department of Mathematics, Tongji University. *Advanced Mathematics*, 6th ed, Beijing,
532Higher Education Press, 2007.
- 533[25] Xu Lizhi, *Modern Mathematics Handbook*, 1st ed, Wuhan: Huazhong University of Science &
534Technology Press, 1999.
- 535[26] A.-M. Gustafsson, L. Westerlund, G. Hellström, CFD-modelling of natural convection in a
536groundwater-filled borehole heat exchanger, *Applied Thermal Engineering* 30 (2010) 683-691.

Figure Captions

- Fig.1 The schematic diagram of groundwater which flows past BGHE
- Fig.2 The comparison between pure conduction and combined heat transfer
- Fig.3 The isothermals with the increase of U
- Fig.4 The isothermals with the increase of Fo
- Fig.5 The mean temperature response with the time when φ adopts different angles
- Fig.6 The mean temperature response with the velocity value when φ adopts different angles
- Fig.7 The schematic diagram of three even-distributed points around BGHE
- Fig.8 Some distributing modes for three points around BGHE
- Fig.9 The distributing diagram while there are different number points
- Fig.10 The mean temperature response along Z -axis
- Fig.11 The temperature responses of three points with U
- Fig.12 The temperature responses of three points with the time
- Fig.13 The temperature responses of three points with the change of orientation
- Fig.14 The variation trend of slopes of three points while U and φ remain changeless
- Fig.15 The variation trend of slope when orientation and velocity intensity varies respectively
- Fig.16 The temperature responses of both model calculation and experiments

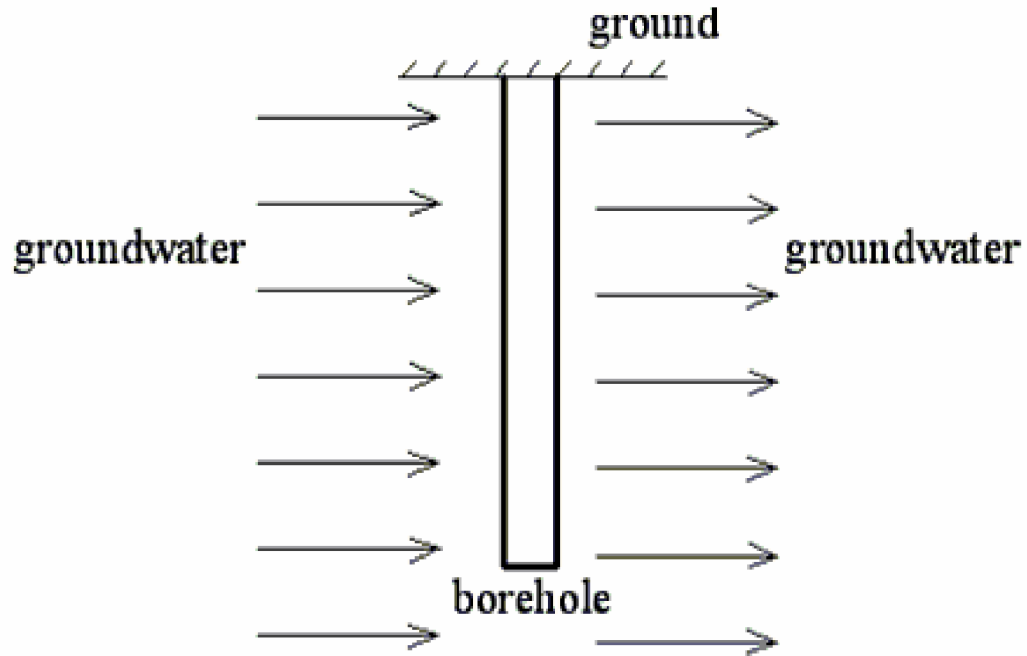


Fig.1 The schematic diagram of groundwater which flows past BGHE

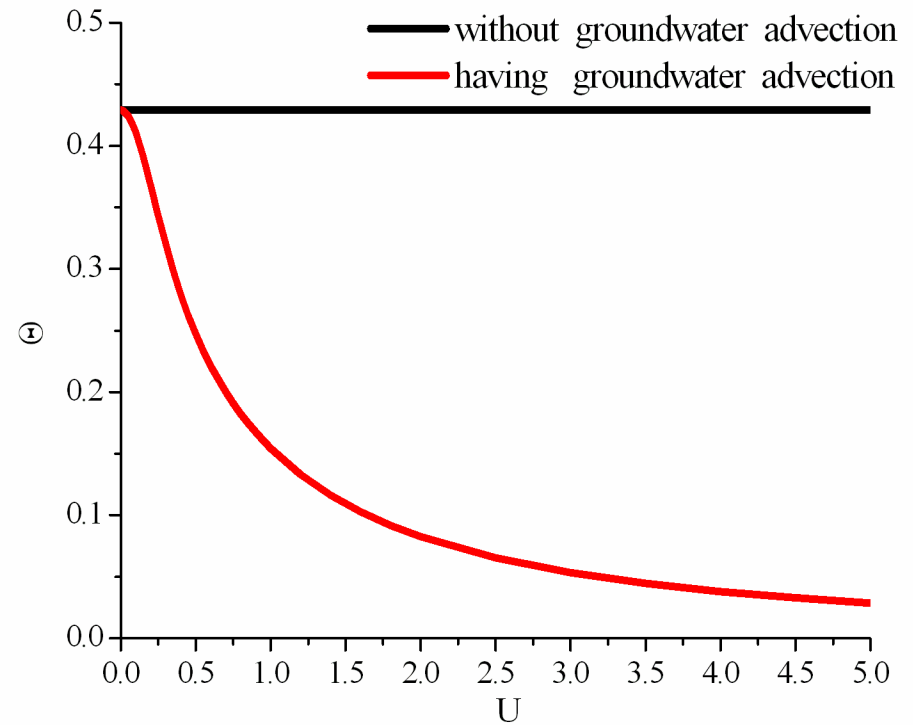
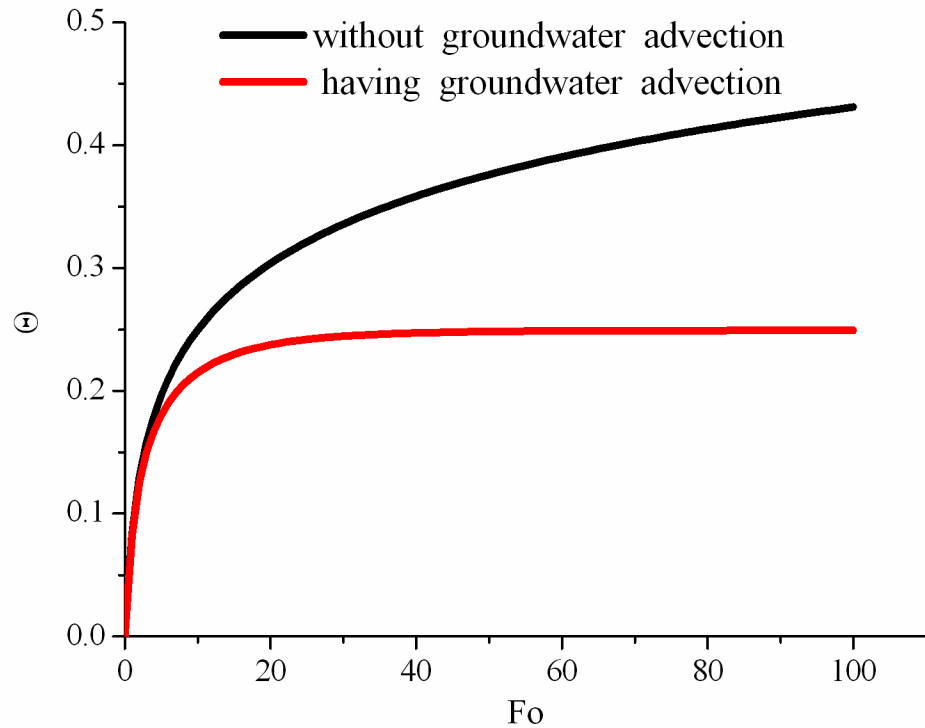


Fig.2 The comparison between pure conduction and combined heat transfer

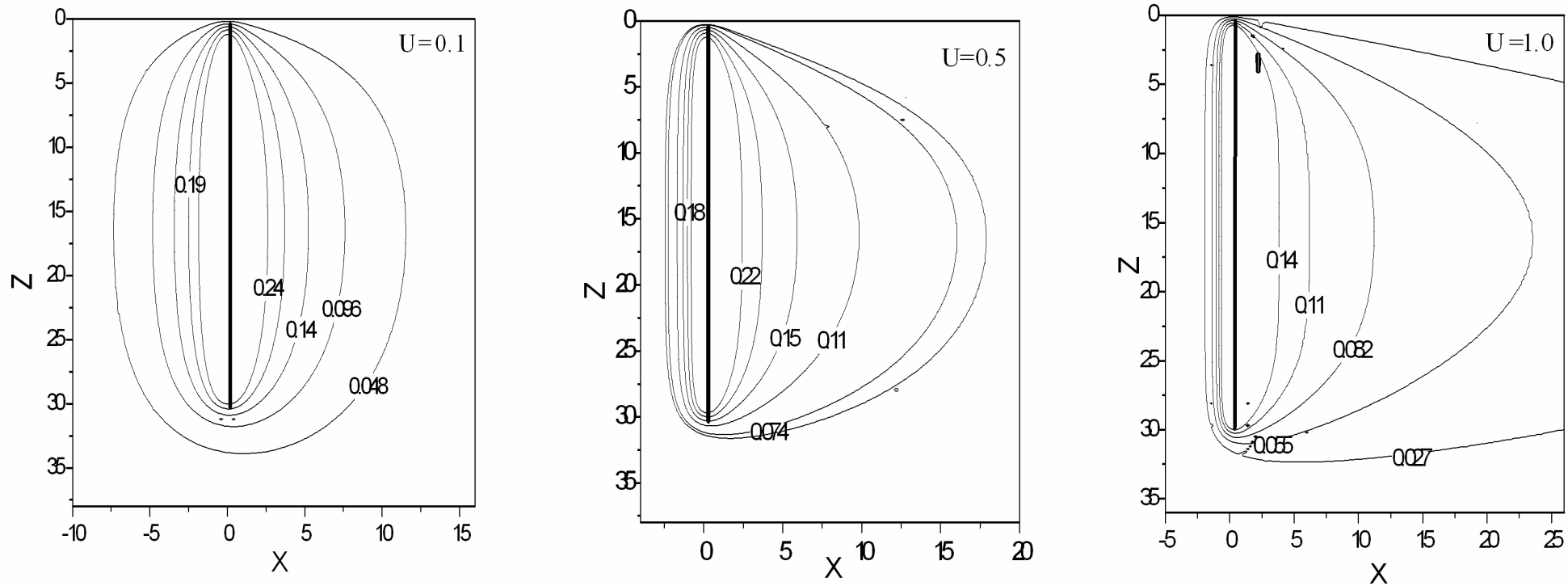


Fig.3 The isothermals with the increase of U

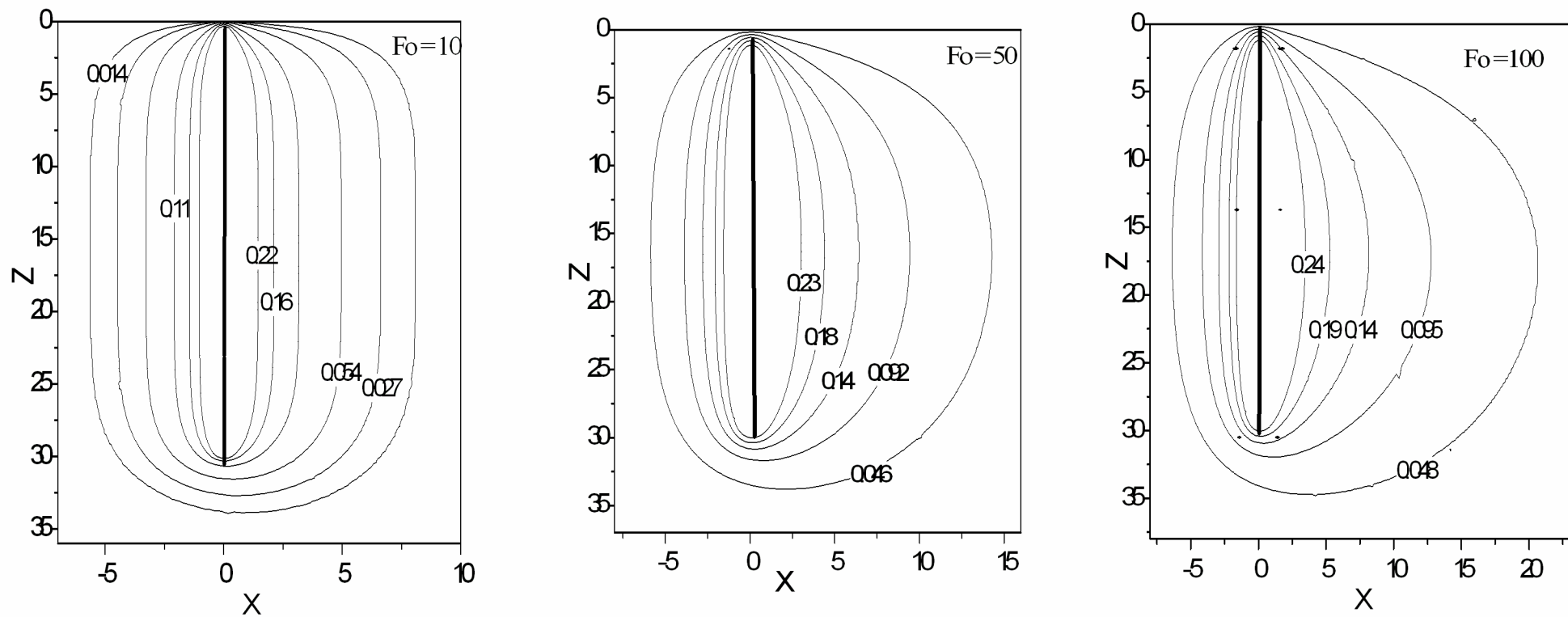


Fig.4 The isothermals with the increase of Fo

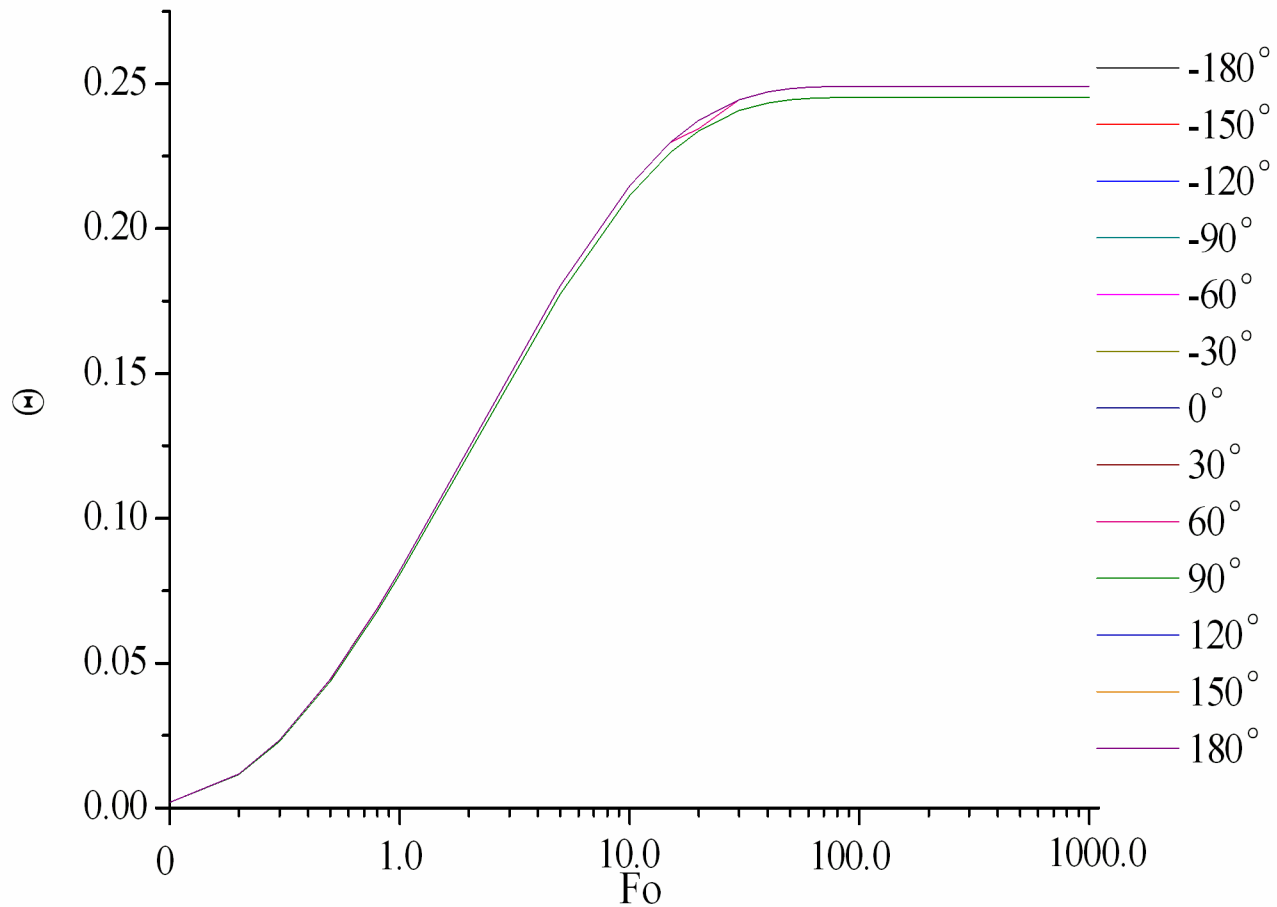


Fig.5 The mean temperature response with the time when φ adopts different angles

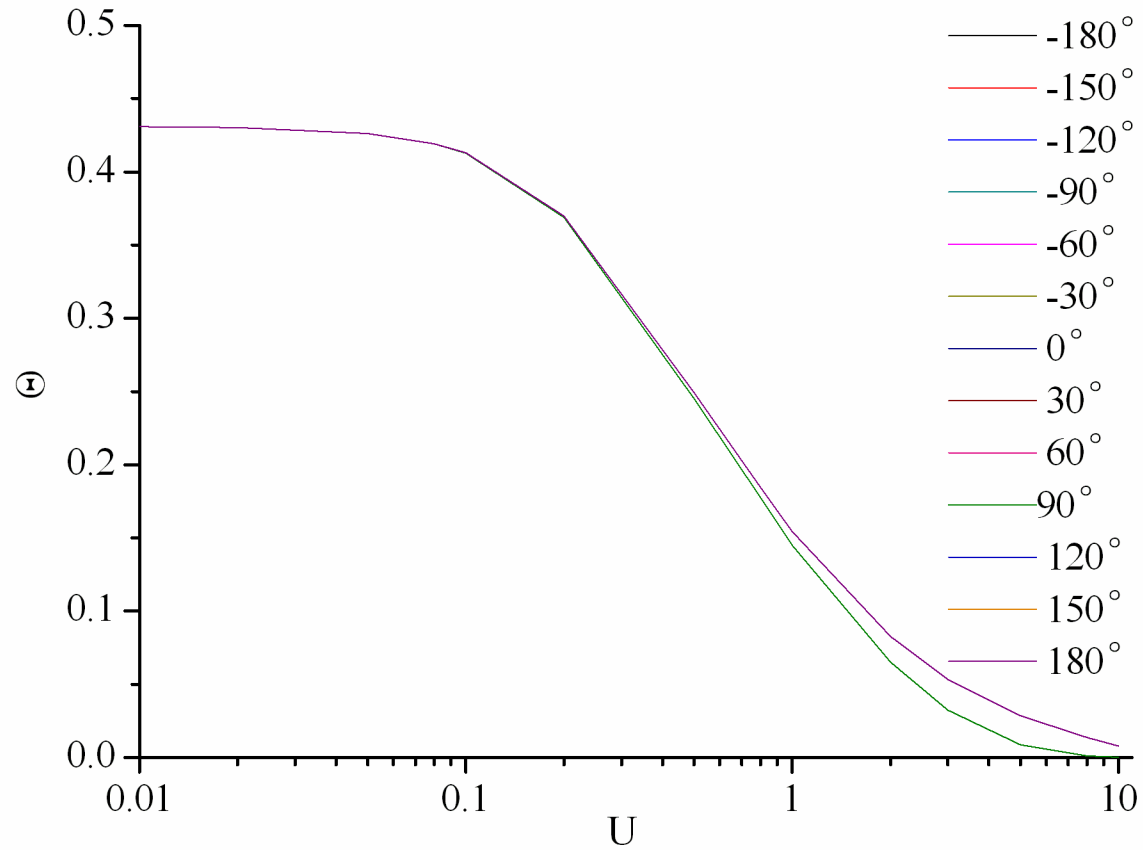


Fig.6 The mean temperature response with the velocity value when φ adopts different angles

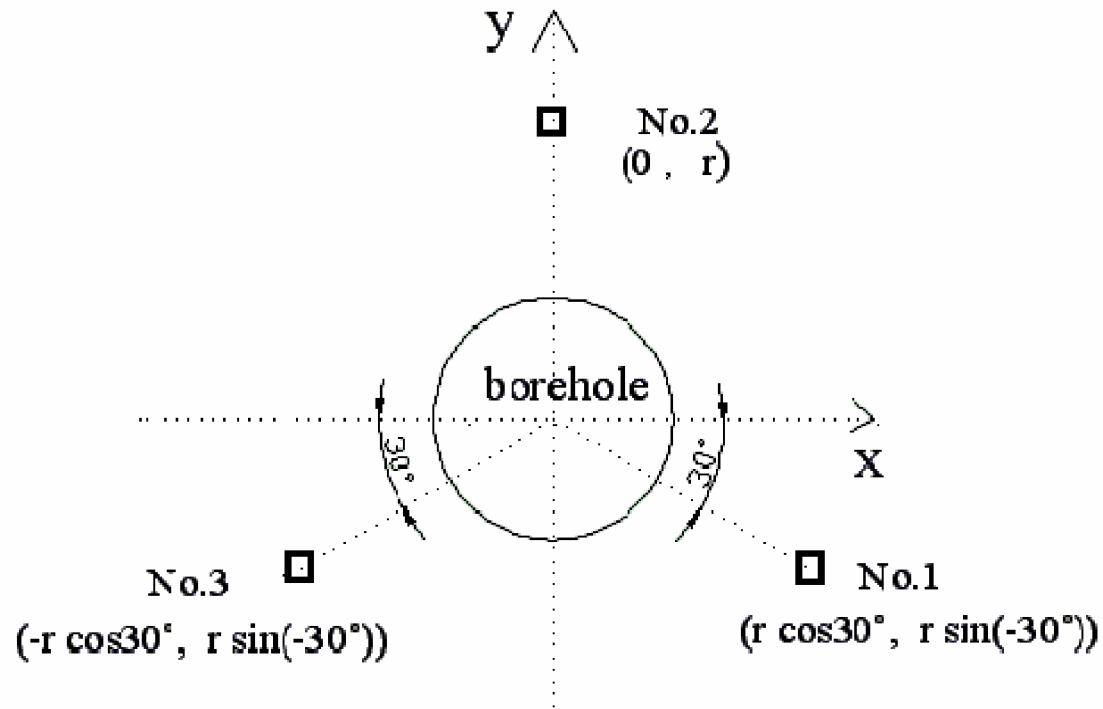


Fig.7 The schematic diagram of three even-distributed points around BGHE

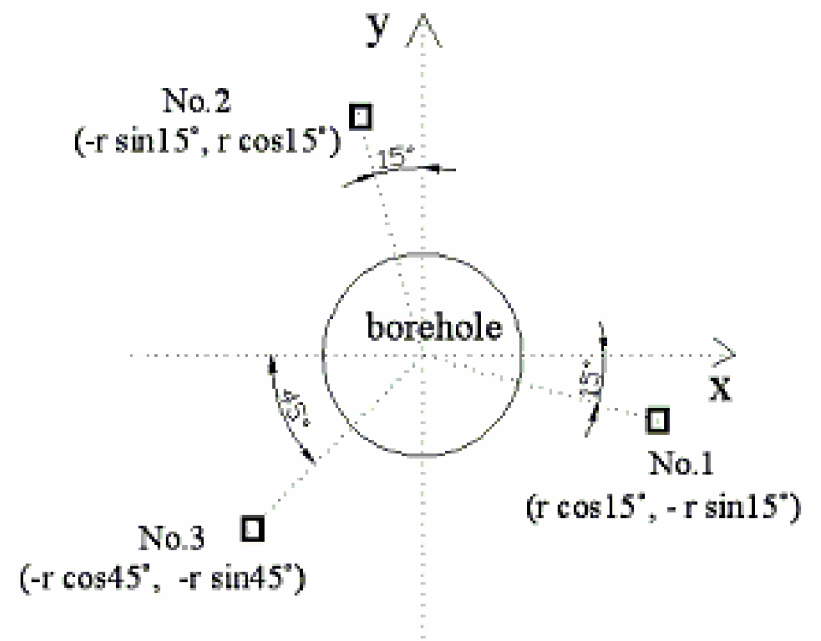
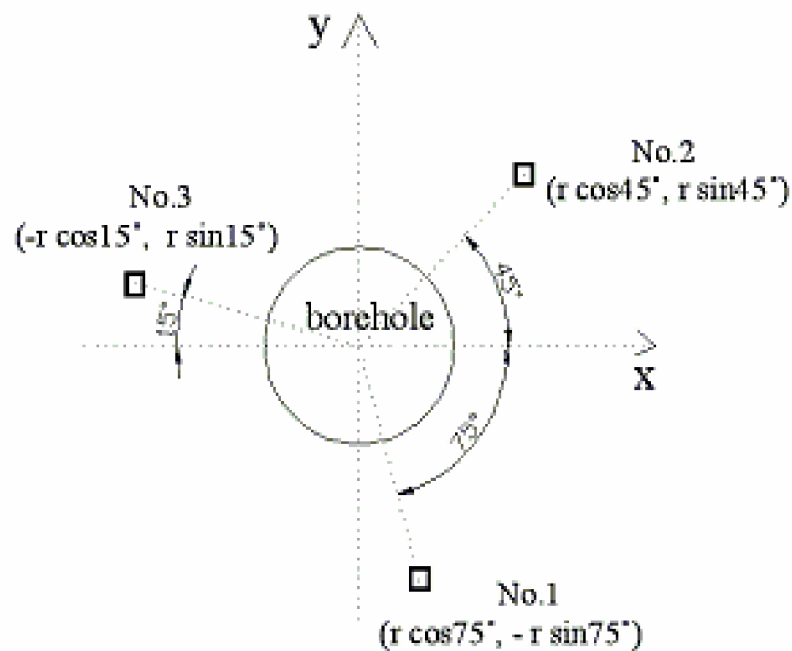
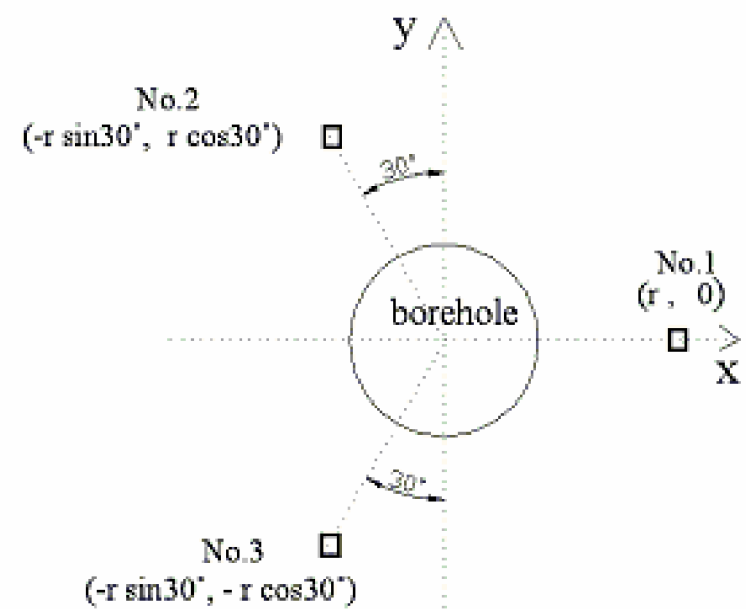
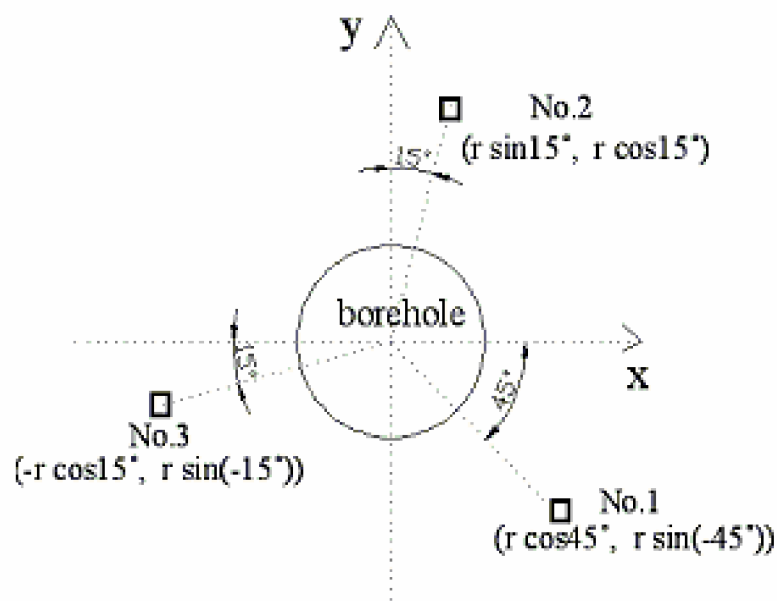


Fig.8 Some distributing modes for three points around BGHE

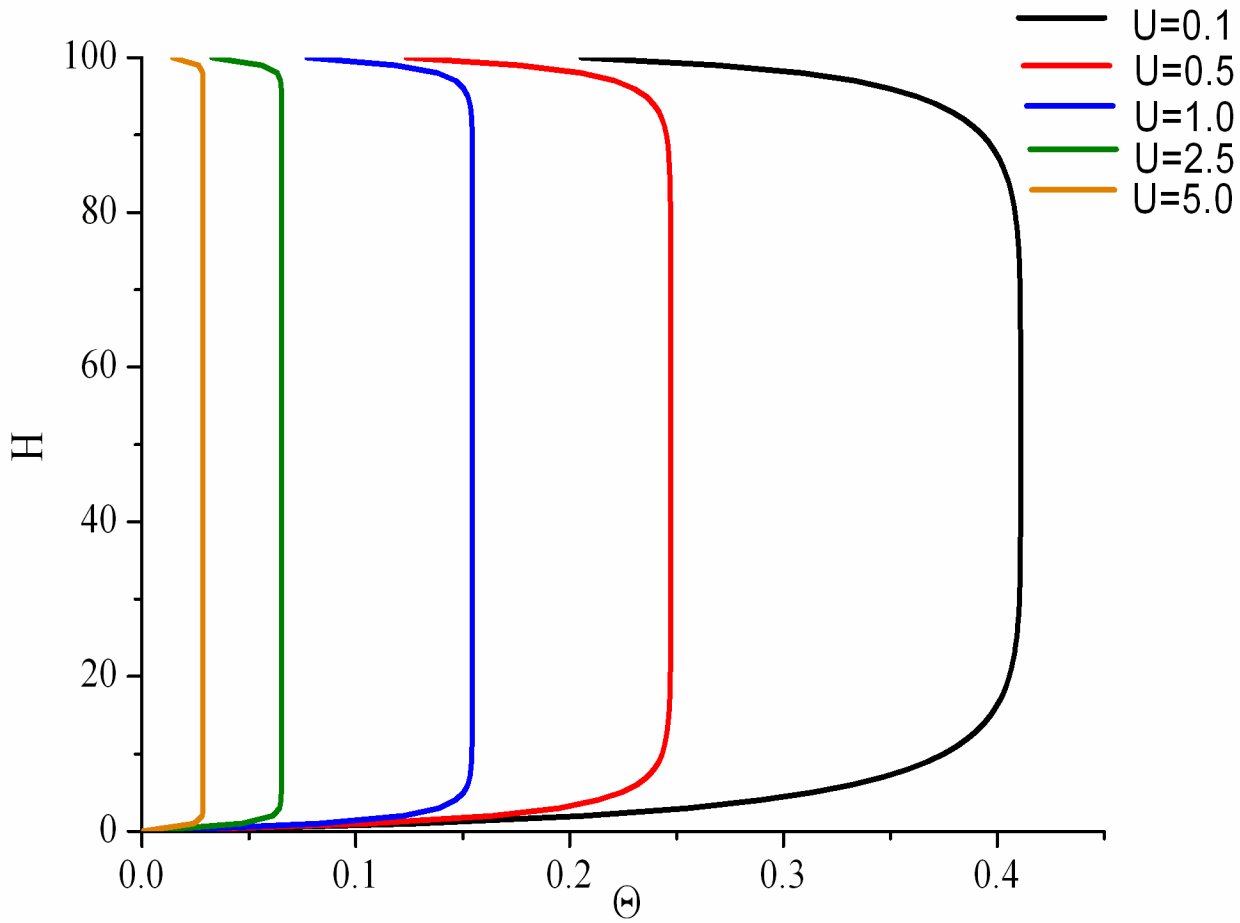


Fig.10 The mean temperature response along Z-axis

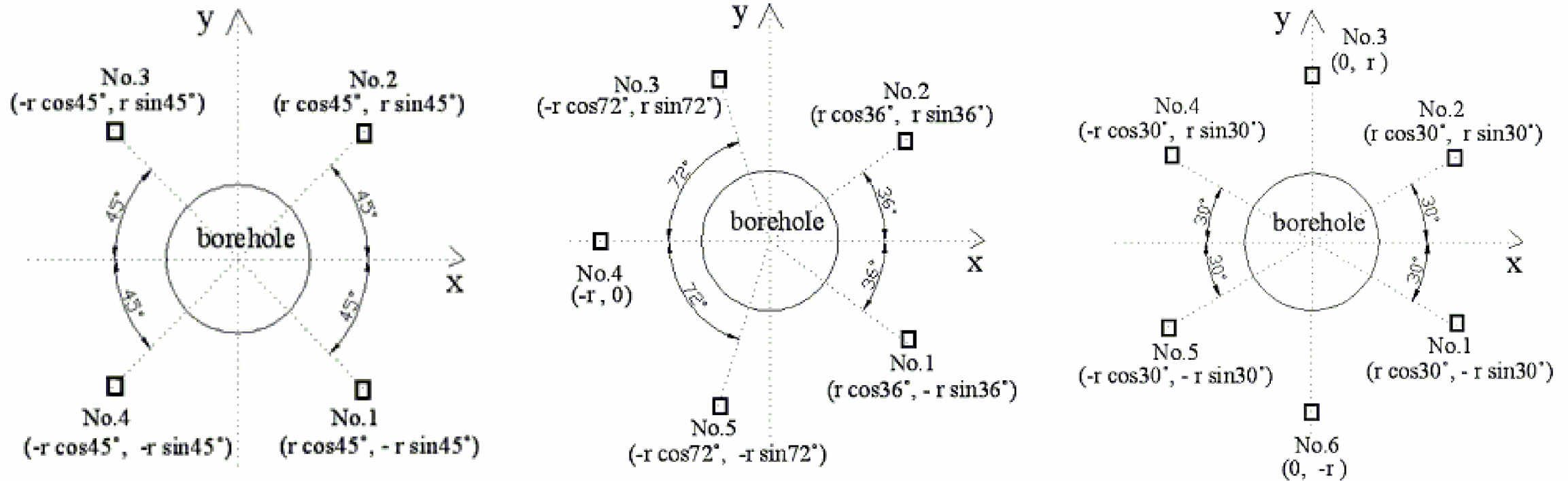


Fig.9 The distributing diagram while there are different number points

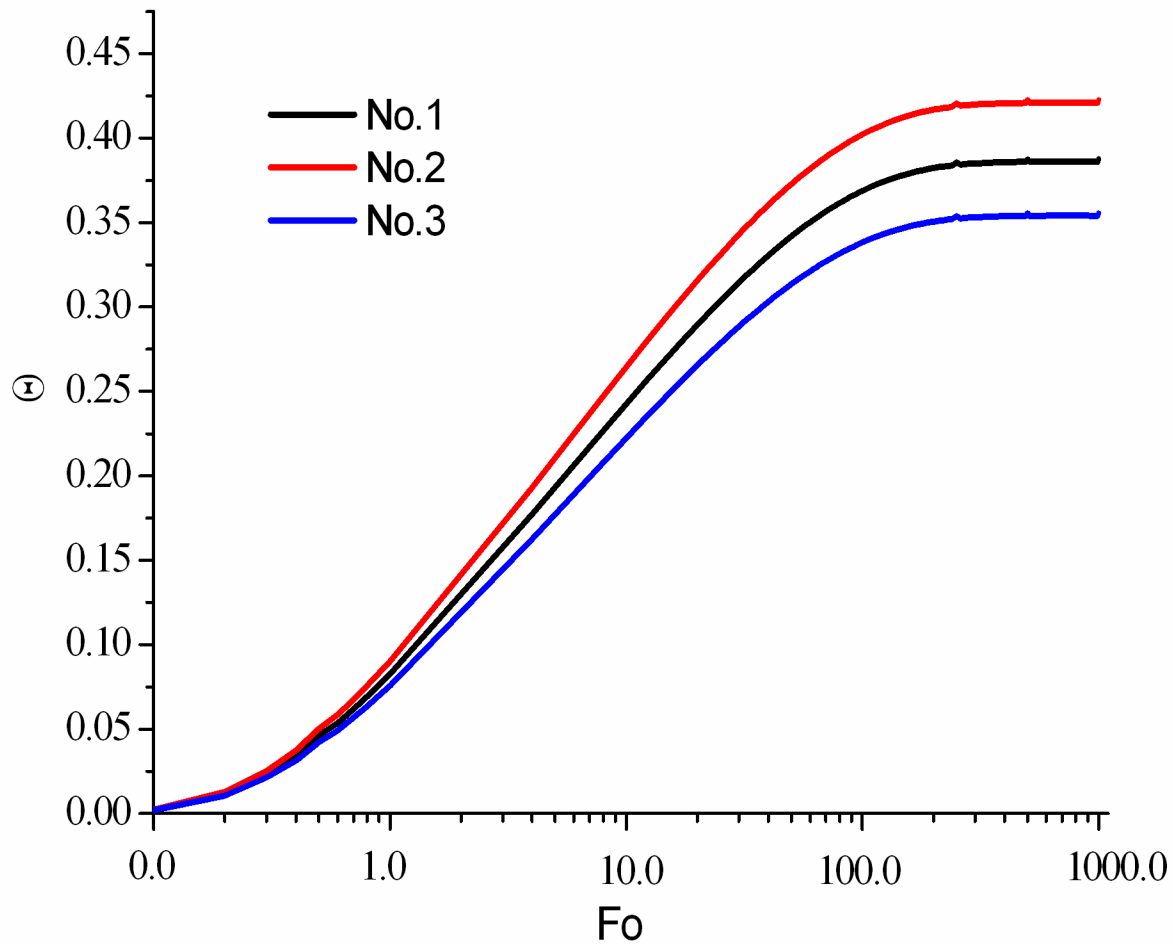


Fig.12 The temperature responses of three points with the time

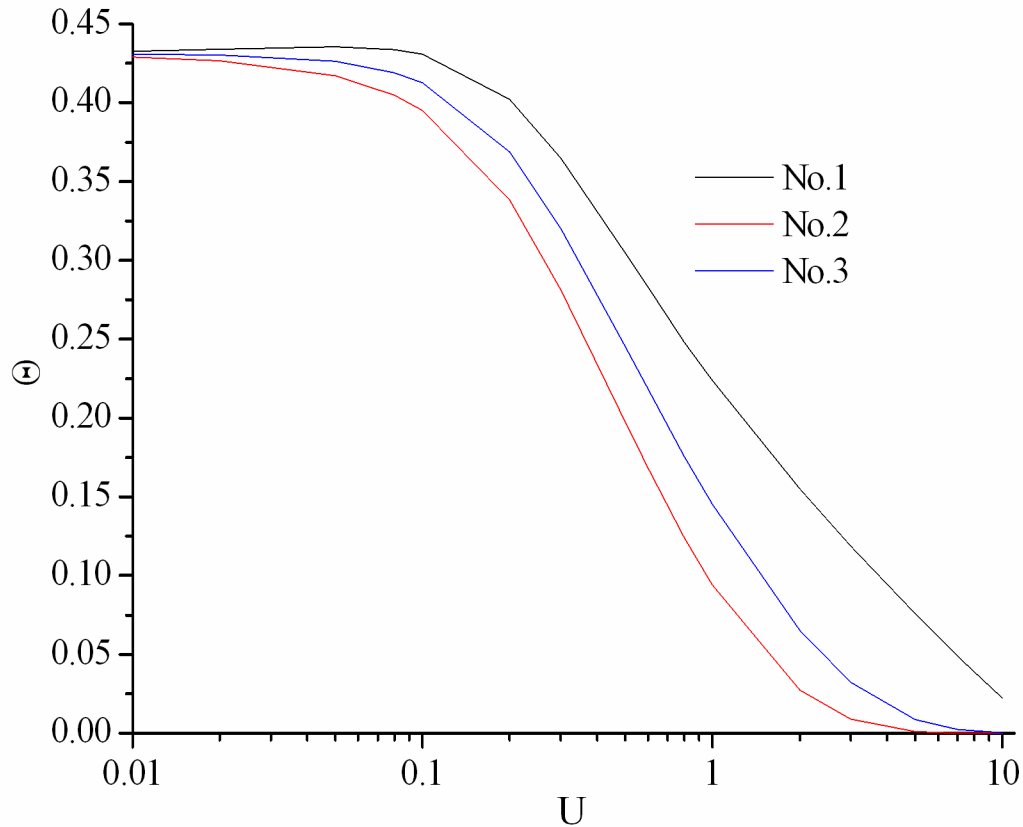


Fig.11 The temperature responses of three points with U

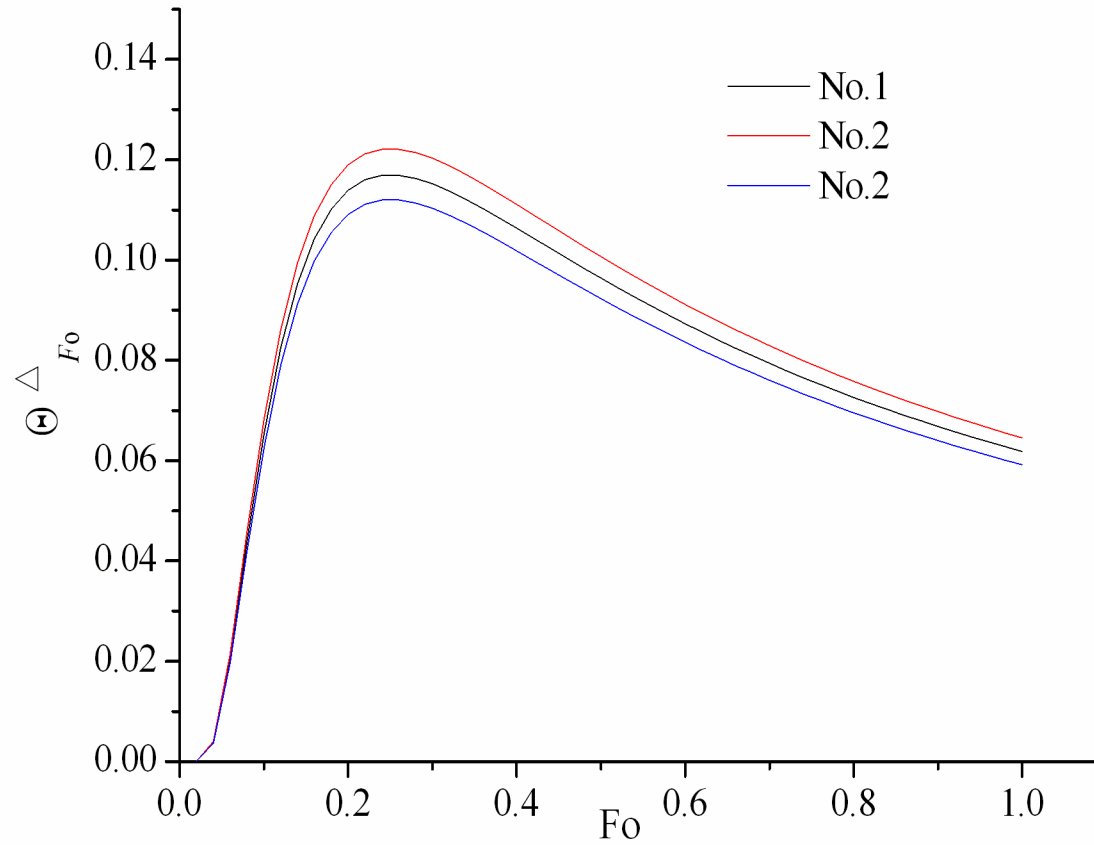


Fig.14 The variation trend of slopes of three pints while U and φ remain changeless

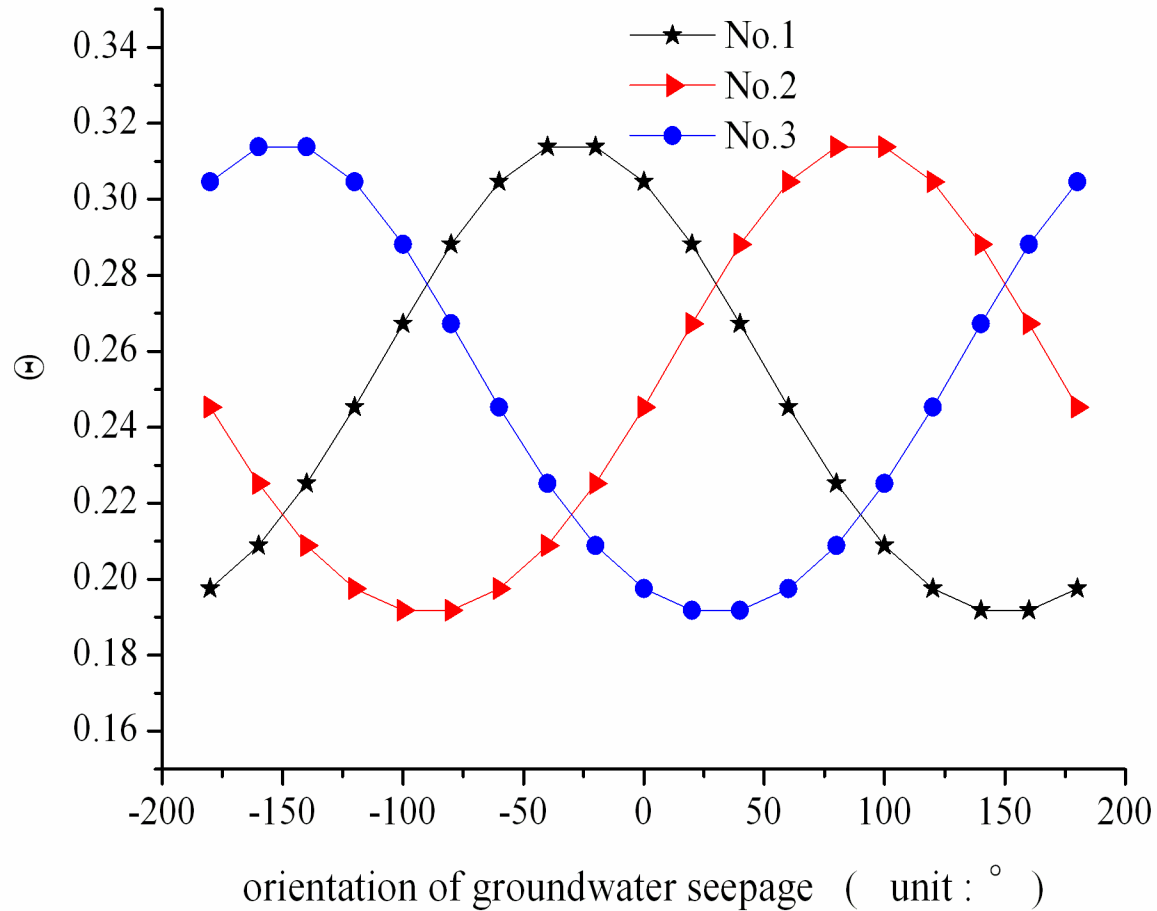


Fig.13 The temperature responses of three points with the change of orientation

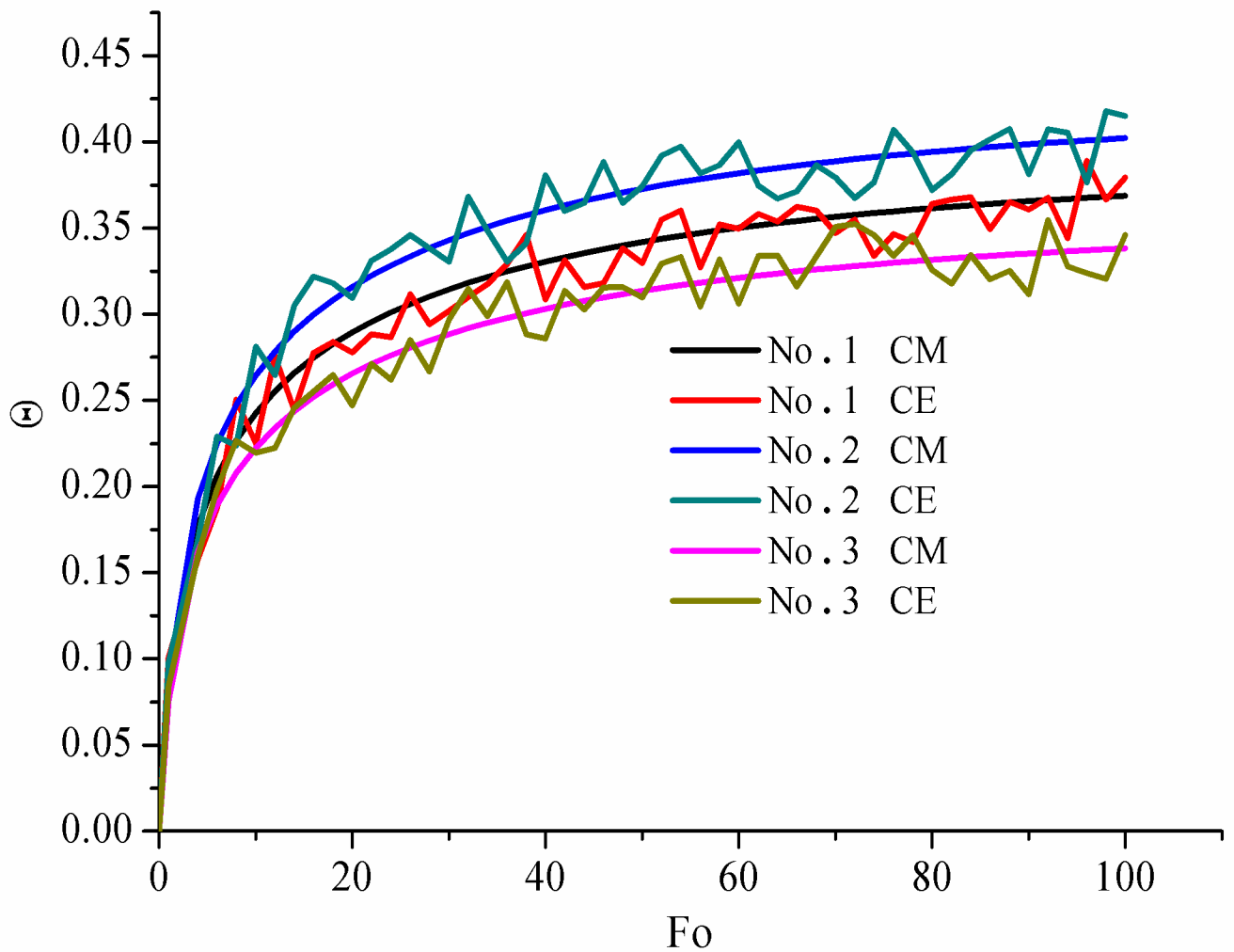


Fig.16 The temperature responses of both model calculation and experiments

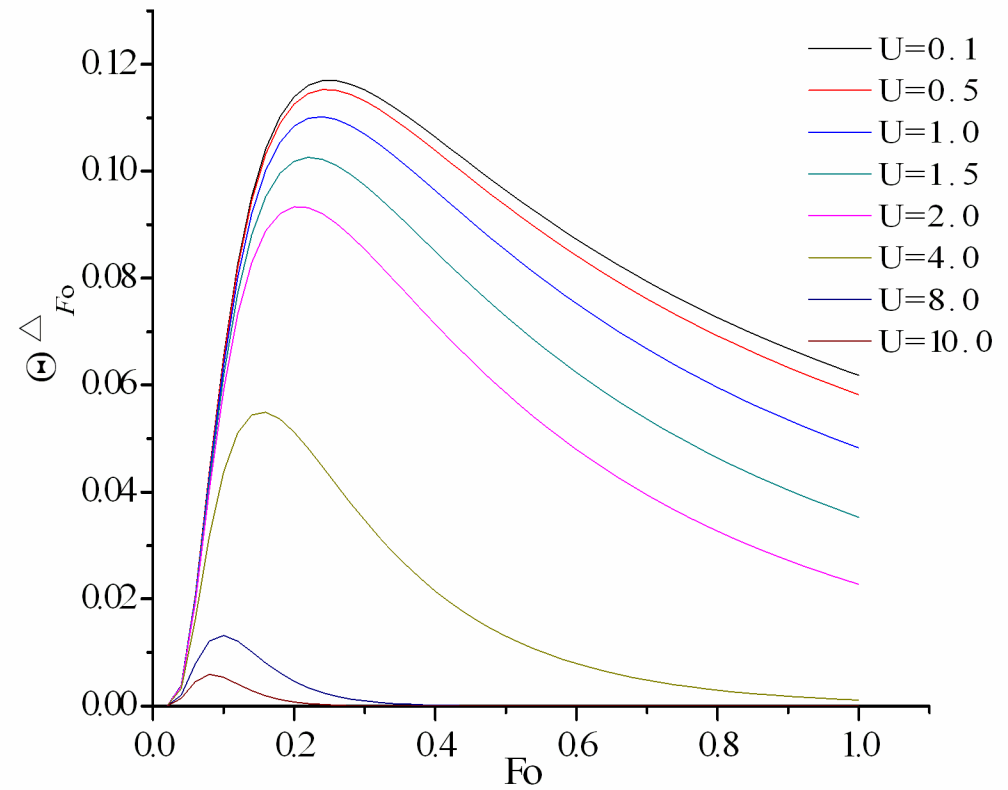
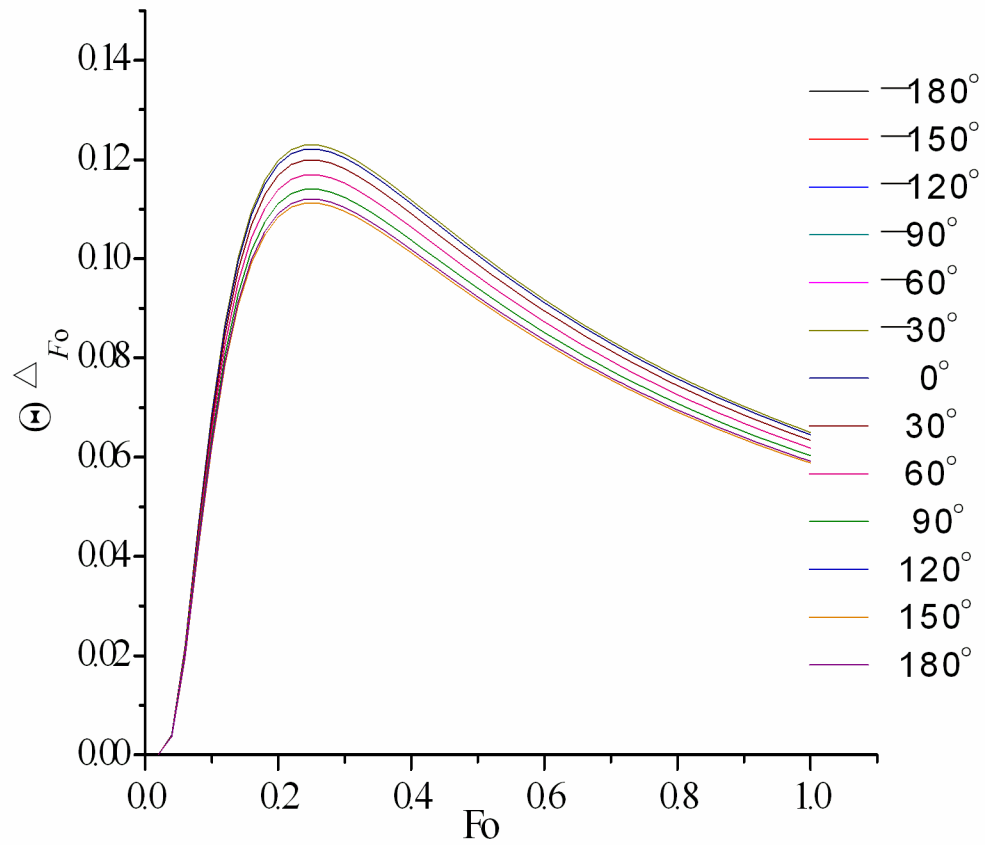


Fig.15 The variation trend of slope when orientation and velocity intensity varies respectively